J|A|C|S
ARTICLES
Published on Web 02/15/2006

Effects of Thioether Substituents on the O_2 Reactivity of β-Diketiminate−Cu(I) Complexes: Probing the Role of the Methionine Ligand in Copper Monooxygenases

Nermeen W. Aboelella, Benjamin F. Gherman, Lyndal M. R. Hill, John T. York, Nicole Holm, Victor G. Young, Jr., Christopher J. Cramer, and William B. Tolman*

Contribution from the Department of Chemistry, Center for Metals in Biocatalysis, and Minnesota Supercomputer Institute, University of Minnesota, 207 Pleasant Street SE, Minneapolis, Minnesota 55455

Received November 23, 2005; E-mail: tolman@chem.umn.edu

Abstract: The activation of dioxygen by dopamine β-monooxygenase (DβM) and peptidylglycine α-hydroxylating monooxygenase (PHM) is postulated to occur at a copper site ligated by two histidine imidazoles and a methionine thioether, which is unusual because such thioether ligation is not present in other O_2-activating copper proteins. To assess the possible role of the thioether ligand in O_2 activation by DβM and PHM, two new ligands comprising β-diketiminates with thioether substituents were synthesized and Cu(I) and Cu(II) complexes were isolated. The Cu(II) compounds are monomeric and exhibit intramolecular thioether coordination. While the Cu(I) complexes exhibit a multinuclear topology in the solid state, variable-temperature ^{1}H NMR studies implicate equilibria in solution, possibly including monomers with intramolecular thioether coordination that are structurally defined by DFT calculations. Low-temperature oxygenation of solutions of the Cu(I) complexes generates stable 1:1 Cu/O_2 adducts, which on the basis of combined experimental and theoretical studies adopt side-on "η^2" structures with negligible Cu−thioether bonding and significant peroxo-Cu(III) character. In contrast to previously reported findings with related ligands lacking the thioether group, however (cf., Aboelella; et al. *J. Am. Chem. Soc.* **2004**, *126*, 16896), purging the solutions of the thioether-containing adducts with argon results in conversion to bis(μ-oxo)dicopper(III) species. A role for the thioether in promoting loss of O_2 from the 1:1 Cu/O_2 adduct and facilitating trapping of the resulting Cu(I) complex to yield the bis(μ-oxo) species is proposed, and the possible relevance of this role to that of the methionine in the active sites of DβM and PHM is discussed.

Introduction

The binding and activation of dioxygen by copper centers is critically important in biology[1] and catalysis.[2] In proteins, such reactions often occur at active sites with multiple copper ions,[3] and studies of model complexes have provided extensive insight into the nature of relevant multicopper−O_2 species.[4] The coordination and reduction of O_2 also occurs at single Cu sites in proteins,[5] as exemplified by dopamine β-monooxygenase (DβM)[5,6] and peptidylglycine α-hydroxylating monooxygenase (PHM).[5,7] These enzymes perform stereospecific hydroxylations of C−H bonds (of dopamine or peptide glycine terminus, respectively) to produce physiologically significant metabolites (norepinephrine or α-amidated peptide). X-ray crystallographic data on PHM[8] and X-ray absorption spectroscopy on DβM[9] and PHM[10] have revealed that these similar proteins contain two copper ions separated by ∼11 Å, one with three imidazolyl ligands (Cu_H) and the other with two imidazoles and a thioether (Cu_M) provided by the respective histidine or methionine side

(1) Selected recent reviews: (a) Solomon, E. I.; Sundaram, U. M.; Machonkin, T. E. *Chem. Rev.* **1996**, *96*, 2563. (b) Solomon, E. I.; Chen, P.; Metz, M.; Lee, S.-K.; Palmer, A. E. *Angew. Chem., Int. Ed.* **2001**, *40*, 4570. (c) Itoh, S. In *Comprehensive Coordination Chemistry II*; McCleverty, J. A., Meyer, T. J., Eds.; Elsevier: Amsterdam, 2004; Vol. 8, pp 369−393. (d) Lee, D.-H.; Lucchese, B.; Karlin, K. D. In *Comprehensive Coordination Chemistry II*; McCleverty, J. A., Meyer, T. J., Eds.; Elsevier: Amsterdam, 2004; Vol. 8, pp 437−457. (e) Halcrow, M. A.; Knowles, P. F.; Phillips, S. E. V. In *Handbook on Metalloproteins*; Bertini, I., Sigel, A., Sigel, H., Eds.; Marcell Dekker: New York, 2001; Chapter 15, pp 709−762.

(2) For recent examples, see: (a) Kirillov, A. M.; Kopylovich, M. N.; Kirillova, M. V.; Haukka, M.; da Silva, M. F. C. G.; Pombeiro, A. J. L. *Angew. Chem., Int. Ed.* **2005**, *44*, 4345 and references therein. (b) Markó, I. E.; Gautier, A.; Dumeunier, R.; Doda, K.; Philippart, F.; Brown, S. M.; Urch, C. J. *Angew. Chem., Int. Ed.* **2004**, *43*, 1588.

(3) Some recent reports: (a) Lieberman, R. L.; Rosenzweig, A. C. *Dalton Trans.* **2005**, 3390. (b) Bento, I.; Martins, L. O.; Lopes, G. G.; Carrondo, M. A.; Lindley, P. F. *Dalton Trans.* **2005**, 3507.

(4) (a) Mirica, L. M.; Ottensaelder, X.; Stack, T. D. P. *Chem. Rev.* **2004**, *104*, 1013. (b) Lewis, E. A.; Tolman, W. B. *Chem. Rev.* **2004**, *104*, 1047. (c) Hatcher, L.; Karlin, K. D. *J. Biol. Inorg. Chem.* **2004**, *9*, 669. (d) Itoh, S.; Fukuzumi, S. *Bull. Chem. Soc. Jpn.* **2002**, *75*, 2081. (e) Kopf, M.-A.; Karlin, K. D. In *Biomimetic Oxidations Catalyzed by Transition Metal Complexes*; Meunier, B., Ed.; Imperial College Press: London, 2000; pp 309−362. (f) Schindler, S. *Eur. J. Inorg. Chem.* **2000**, 2311. (g) Blackman, A. G.; Tolman, W. B. *Struct. Bonding (Berlin)* **2000**, *97*, 179.

(5) (a) Klinman, J. P. *Chem. Rev.* **1996**, *96*, 2541. (b) Halcrow, M. A. In *Comprehensive Coordination Chemistry II*; McCleverty, J. A., Meyer, T. J., Eds.; Elsevier: Amsterdam, 2004; Vol. 8, pp 395−436.

(6) Stewart, L. C.; Klinman, J. P. *Annu. Rev. Biochem.* **1988**, *57*, 551.

(7) Eipper, B. A.; Stoffers, D. A.; Mains, R. E. *Annu. Rev. Neurosci.* **1992**, *15*, 57.

(8) (a) Prigge, S. T.; Kolhekar, A. S.; Eipper, B. A.; Mains, R. E.; Amzel, L. M. *Science* **1997**, *278*, 1300. (b) Prigge, S. T.; Kolhekar, A. S.; Eipper, B. A.; Mains, R. E.; Amzel, L. M. *Nat. Struct. Biol.* **1999**, *6*, 976. (c) Prigge, S. T.; Eipper, B. A.; Mains, R. E.; Amzel, L. M. *Science* **2004**, *304*, 864.

(9) (a) Scott, R. A.; Sullivan, R. J.; DeWolf, W. E. J.; Dolle, R. E.; Kruse, L. I. *Biochemistry* **1988**, *27*, 5411. (b) Reedy, B. J.; Blackburn, N. J. *J. Am. Chem. Soc.* **1994**, *116*, 1924. (c) Blackburn, N. J.; Hasnain, S. S.; Pettingill, T. M.; Strange, R. W. *J. Biol. Chem.* **1991**, *266*, 23120.

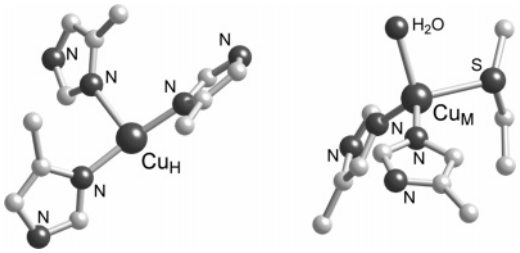

Figure 1. The copper sites in PHM as determined by X-ray crystallography.[8a] The water molecules on Cu_H are not shown. Cu_M is the presumed site of dioxygen binding and reduction and is located ~11.5 Å from Cu_H.

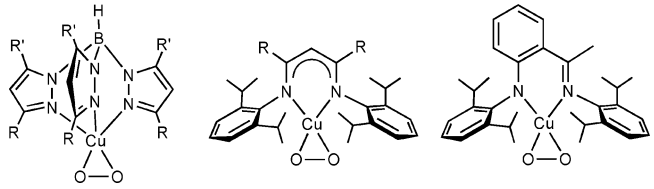

Figure 2. Structurally characterized 1:1 Cu/O_2 adducts.[18,19] Ad = adamantyl.

chains (Figure 1). Various evidence supports the notion that O_2 coordinates to Cu_M during the enzymes' catalytic cycles,[9b,10b] including an X-ray crystal structure of an end-on Cu_M-O_2 adduct generated when a reduced Cu(I) form of PHM was treated with O_2 in the presence of a slow substrate.[8c] Recently proposed mechanisms invoke this or related Cu_M-O_2 adducts as the species directly responsible for attacking the C−H bond of the substrate, although there are differences of opinion regarding later reaction steps.[11−14]

The binding and activation of O_2 at a Cu(I) center supported by a thioether ligand as proposed for DβM and PHM is unusual, because such thioether ligation is not present in other O_2-activating copper proteins[1] and is instead typically associated with "type 1" electron-transfer sites.[15] Several different roles for the methionine ligand in catalysis by DβM and PHM have been suggested. For example, preferential stabilization of the Cu(I) state of Cu_M by the methionine ligand has been proposed to increase the driving force for electron transfer from Cu_H to Cu_M.[8b] Such stabilization of the Cu(I) state has also been suggested to decrease the equilibrium constant for O_2 binding to Cu_M, thus preventing "leakage" of reactive oxygen intermediates by ensuring that O_2 reduction does not occur in the absence of substrate.[11,12] These notions are supported by the observation by EXAFS[10c] and theory[12] of a shorter Cu_M-S(Met) bond distance in the Cu(I) form relative to the Cu(II) state. It has also been hypothesized that the methionine ligand stabilizes a putative $Cu(II)_M-$oxyl intermediate, which is suggested to form after C−H bond activation by the Cu_M-O_2 species.[12] These proposals for the role of the methionine ligand are intuitively appealing, yet they are provocative and deserve testing.

In synthetic chemistry, examples of thioether coordination in complexes of Cu(I) and Cu(II) abound,[16] but in no case have Cu(I) complexes with thioether ligands been found to yield isolable Cu/O_2 intermediates upon oxygenation.[17] Mononuclear Cu/O_2 complexes are typically only observed as transient intermediates in rapid kinetics studies due to their tendency to form peroxo- and/or bis(μ-oxo)dicopper complexes,[4] but a few such species have been isolated and subjected to structural, spectroscopic, and theoretical characterization. The best characterized are similar insofar as they feature sterically hindered N-donor ligands and side-on "η^2" coordination of the O_2 moiety (Figure 2), but they differ with respect to their electronic structures.[18−20] Complex **1** is best formulated as a Cu(II)−superoxide species,[18b,20a] whereas the strong electron-donating capabilities of the β-diketiminate [$(R_2L^{iPr2})^-$, R = Me or *t*Bu][21] or anilido-imine ligands in **2a** and **2b**, respectively, underly significant Cu(III)−peroxide character in these complexes.[19,20] The steric bulk of $(R_2L^{iPr2})^-$ is critical for isolation of **2a**, because reducing the size of the arene substituents instead results in the generation of bis(μ-oxo)dicopper complexes.[19a,22] The binding of O_2 to $Me_2L^{iPr2}Cu$(MeCN) to yield **2a** is irreversible at low temperature, such that purging solutions with argon removes free O_2 but does not perturb **2a**, thus allowing it to be used subsequently in reactions with other reduced metal species to generate dicopper complexes with different supporting ligands on each metal and/or heterobimetallic complexes.[19b,23] While complexes **1** and **2** represent important models of how O_2 coordination to a single copper site in a protein might occur, both lack the thioether coordination implicated in DβM and PHM.

We hypothesized that replacement of one of the isopropyl substituents in $(Me_2L^{iPr2})^-$ with a thioether appendage would yield a ligand that provides the N_2S(thioether) donor set found in DβM and PHM. Moreover, we envisioned that a 1:1 Cu/O_2 adduct supported by such a N_2S(thioether) donor set (akin to

(10) (a) Eipper, B. A.; Quon, A. S. W.; Mains, R. E.; Boswell, J. S.; Blackburn, N. J. *Biochemistry* **1995**, *34*, 2857. (b) Boswell, J. S.; Reddy, B. J.; Kulathila, R.; Merkler, D.; Blackburn, N. J. *Biochemistry* **1996**, *35*, 12241. (c) Blackburn, N. J.; Rhames, F. C.; Ralle, M.; Jaron, S. *J. Biol. Inorg. Chem.* **2000**, *5*, 341.
(11) Evans, J. P.; Ahn, K.; Klinman, J. P. *J. Biol. Chem.* **2003**, *278*, 49691.
(12) Chen, P.; Solomon, E. I. *J. Am. Chem. Soc.* **2004**, *126*, 4991.
(13) Kamachi, T.; Kihara, N.; Shiota, Y.; Yoshizawa, K. *Inorg. Chem.* **2005**, *44*, 4226.
(14) Gherman, B. F.; Heppner, D. E.; Tolman, W. B.; Cramer, C. J. *J. Biol. Inorg. Chem.* **2006**, *11*, in press.
(15) (a) Gray, H. B.; Malmstrom, B. G.; Williams, R. J. P. *J. Biol. Inorg. Chem.* **2000**, 551. (b) Randall, D. W.; Gamelin, D. R.; LaCroix, L. B.; Solomon, E. I. *J. Biol. Inorg. Chem.* **2000**, *5*, 16.
(16) (a) Bouwman, E.; Driessen, W. L.; Reedijk, J. *Coord. Chem. Rev.* **1990**, *104*, 143. (b) Zanello, P. *Comments Inorg. Chem.* **1988**, *8*, 45.
(17) The following are examples of air-sensitive Cu(I) complexes with thioether ligands that nonetheless do not yield isolable Cu/O_2 intermediates: (a) Casella, L.; Gullotti, M.; Bartosek, M.; Pallanza, G.; Laurenti, E. *J. Chem. Soc., Chem. Commun.* **1991**, 1235. (b) Champloy, F.; Benali-Cherif, N.; Bruno, P.; Blain, I.; Pierrot, M.; Reglier, M.; Michalowicz, A. *Inorg. Chem.* **1998**, *37*, 3910.
(18) (a) Fujisawa, K.; Tanaka, M.; Moro-oka, Y.; Kitajima, N. *J. Am. Chem. Soc.* **1994**, *116*, 12079. (b) Chen, P.; Root, D. E.; Campochiaro, C.; Fujisawa, K.; Solomon, E. I. *J. Am. Chem. Soc.* **2003**, *125*, 466.
(19) (a) Spencer, D. J. E.; Aboelella, N. W.; Reynolds, A. M.; Holland, P. L.; Tolman, W. B. *J. Am. Chem. Soc.* **2002**, *124*, 2108. (b) Aboelella, N. W.; Lewis, E. A.; Reynolds, A. M.; Brennessel, W. W.; Cramer, C. J.; Tolman, W. B. *J. Am. Chem. Soc.* **2002**, *124*, 10660. (c) Aboelella, N. W.; Kryatov, S. V.; Gherman, B. F.; Brennessel, W. W.; Young, V. G., Jr.; Sarangi, R.; Rybak-Akimova, E. V.; Hodgson, K. O.; Hedman, B.; Solomon, E. I.; Cramer, C. J.; Tolman, W. B. *J. Am. Chem. Soc.* **2004**, *126*, 16896. (d) Reynolds, A. M.; Gherman, B. F.; Cramer, C. J.; Tolman, W. B. *Inorg. Chem.* **2005**, *44*, 6989.
(20) (a) Cramer, C. J.; Tolman, W. B.; Theopold, K. H.; Rheingold, A. L. *Proc. Natl. Acad. Sci. U.S.A.* **2003**, *100*, 3635. (b) Gherman, B. F.; Cramer, C. J. *Inorg. Chem.* **2004**, *43*, 7281.
(21) Ligand abbreviations used here are similar to those described previously.[22] Thus, $(R_2L^{R',R''})^-$ refers to a β-diketiminate where R refers to the α-backbone substituents and R′ and R″ refer to the ortho substituents on the aryl ring. Thus, in **2a** for R = Me, the ligand is $(Me_2L^{iPr2})^-$. For simplicity, we denote the more asymmetric ligands in Scheme 1 as $(Me_2L^{iPr,SMe})^-$ or $(Me_2L^{iPr,SPh})^-$.
(22) Spencer, D. J. E.; Reynolds, A. M.; Holland, P. L.; Jazdzewski, B. A.; Duboq-Toia, C.; Pape, L. L.; Yokota, S.; Tachi, Y.; Itoh, S. *Inorg. Chem.* **2002**, *41*, 6307.
(23) Aboelella, N. W.; York, J. T.; Reynolds, A. M.; Fujita, K.; Kinsinger, C. R.; Cramer, C. J.; Riordan, C. G.; Tolman, W. B. *Chem. Commun.* **2004**, 1716.

Scheme 1

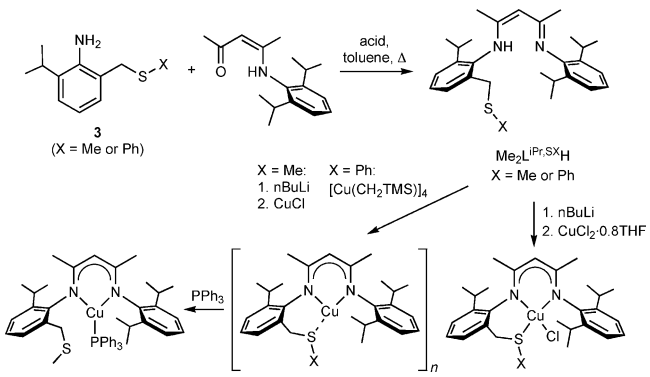

the proposed reactive species in the enzymes) would be accessible, given the precedent provided by the O_2 chemistry of $Me_2L^{iPr2}Cu(MeCN)$[19a−c] and the steric bulk provided by the three remaining ortho-isopropyl group substituents of the new ligands. Studies of such an adduct would enable comparisons with **2** aimed at discerning the role of the thioether in dioxygen binding and activation. Herein, we report the synthesis of two variants of this new ligand, characterization of their complexes with Cu(I) and Cu(II) that demonstrate thioether binding to the metal, and the results of experimental and theoretical studies of the oxygenation reactions of the Cu(I) complexes. Through this work, important effects of the thioether group on the Cu(I)/O_2 chemistry have been identified that are relevant to the possible role of the methionine ligand in O_2 activation by DβM and PHM.[24]

Results and Discussion

Ligand Synthesis and Characterization. The β-diketimines $Me_2L^{iPr,SX}H$ (X = Me or Ph; Scheme 1) were targeted for use as precursors of β-diketiminate ligands for coordination to Cu(I) and Cu(II) ions. In addition to containing ortho isopropyl substituents that we hoped would sterically favor monocopper complex formation, the ligands feature a methylene linker between the phenyl ring and the thioether sulfur that would result in the formation of a favorable six-membered chelate ring upon intramolecular binding of the thioether to a coordinated metal ion. We prepared $Me_2L^{iPr,SX}H$ (R = Me or Ph) by condensing the thioether-substituted anilines **3** (X = Me, known;[25] X = Ph, prepared by an analogous procedure[26]) with 2-(2,6-diisopropylphenylimido)-2-pentene-4-one[27] (Scheme 1). The compound $Me_2L^{iPr,SPh}H$ was isolated as an analytically pure, crystalline solid in modest yield (33%) and was fully characterized, including by X-ray diffraction (Figure S1, Supporting Information). Deprotonation of $Me_2L^{iPr,SPh}H$ with ^{n}BuLi to yield the β-diketiminate $Li(Me_2L^{iPr,SPh})$ was possible (^{1}H NMR), but isolation of the product was hindered by its high solubility in organic solvents. Thus, we used either freshly prepared crude solutions of $Li(Me_2L^{iPr,SPh})$ or the precursor $Me_2L^{iPr,SPh}H$ itself to prepare copper complexes (see below).

The synthesis of $Me_2L^{iPr,SMe}H$ was problematic, as the condensation reaction afforded a mixture of the desired product and the symmetric species $Me_2L^{iPr2}H$ and $Me_2L^{SMe2}H$ according to ^{1}H and $^{13}C\{^1H\}$ NMR spectroscopy and mass spectrometry. The ratio of these products was ~45:45:10 (^{1}H NMR) and could be improved to ~6:3:1 by crystallization of the crude product from EtOH. Treatment of the mixture with ^{n}BuLi resulted in the selective precipitation of $Li(Me_2L^{iPr,SMe})$ that was subsequently used for the preparation of copper complexes (see below).

Notable features of the ^{1}H NMR spectra of the β-diketimines $Me_2L^{iPr,SX}H$ (X = Me or Ph) include a singlet at ~12.5 ppm corresponding to the −N*H* proton and an AB pattern for the diastereotopic methylene protons of the thioether arm (e.g., for R = Me, δ = 3.68 and 3.58 ppm, J = 13.2 Hz). For $Li(Me_2L^{iPr,SMe})$, the −N*H* resonance is absent and the chemical shift difference between the thioether methylene resonances increases significantly to ~0.5 ppm, with two doublets observed (an AX pattern). Similarly, large differences in the chemical shifts of the diastereotopic methylene hydrogens were observed in the copper complexes of the ligands (see below).

Synthesis and Characterization of Cu(II) Complexes. Copper(II) complexes of the ligands $(Me_2L^{iPr,SX})^-$ were prepared to probe the coordinating ability of the thioether appendage, in particular to assess whether intramolecular binding would occur to an oxidized copper site such as that which would be formed upon oxygenation of a Cu(I) precursor. Using procedures analogous to those reported previously for the preparation of $[LCuCl]_n$ (L = β-diketiminate, n = 1 or 2),[19a,22,28,29] solutions of the lithium salts $Li(Me_2L^{iPr,SX})$ in THF were added to a slurry of $CuCl_2$·0.8THF in THF (Scheme 1). The dark purple complexes $Me_2L^{iPr,SX}CuCl$ were isolated in modest yields (~50%) after crystallization from toluene/pentane mixtures at −20 °C.

The X-ray crystal structures of both Cu(II) complexes indicate that they are monomeric species in the solid state (Figure 3). This observation attests to a degree of steric bulk imposed by $(Me_2L^{iPr,SX})^-$ that is similar to that of $(Me_2L^{iPr2})^-$, which supports a 3-coordinate monomeric geometry in $Me_2L^{iPr2}CuCl$.[28] Other β-diketiminates with smaller arene and/or backbone substituents yield chloride-bridged dimeric structures, $[LCu(\mu\text{-}Cl)]_2$, in the solid state.[29] The thioether sulfur atom is bound to the Cu(II) center in both complexes, with a Cu−S bond distance of 2.3793(11) Å in $Me_2L^{iPr,SMe}CuCl$ and 2.5941(9) Å in $Me_2L^{iPr,SPh}CuCl$, which contains the more bulky phenyl group on the thioether arm. These Cu(II)−thioether bond distances fall within the range of such distances reported previously (2.28−2.91 Å, avg = 2.41 Å).[30] The thioether coordination results in a significant distortion of the copper geometry away from the trigonal planar topology of $Me_2L^{iPr2}CuCl$,[28] such that the chloride ligand lies below the N−Cu−N plane (by 30.1° or 24.7° for X = Me or Ph, respectively) and has a longer bond to the Cu(II) ion (X = Me, 2.218(1) Å; X = Ph, 2.1846(9) Å) than in the 3-coordinate complex (2.127(1) Å). Overall, the distorted tetrahedral geometries in the complexes $Me_2L^{iPr,SX}$-

(24) Aspects of this work are reported in: Aboelella, N. W. Ph.D. Thesis, University of Minnesota, 2005.
(25) Teramoto, S.; Tanaka, M.; Shimizu, H.; Fujioka, T.; Tabusa, F.; Imaizumi, T.; Yoshida, K.; Fujiki, H.; Mori, T.; Sumida, T.; Tominaga, M. *J. Med. Chem.* **2003**, *46*, 3033.
(26) (a) Gassman, P. G.; Gruetzmacher, G. D. *J. Am. Chem. Soc.* **1974**, *96*, 5487. (b) Gassman, P. G.; Drewes, H. R. *J. Am. Chem. Soc.* **1974**, *96*, 3002.
(27) Dove, A. P.; Gibson, V. C.; Marshall, E. L.; White, A. J. P.; Williams, D. J. *Dalton Trans.* **2004**, 570.
(28) Holland, P. L.; Tolman, W. B. *J. Am. Chem. Soc.* **1999**, *121*, 7270.
(29) Jazdzewski, B. A.; Holland, P. L.; Pink, M.; Young, V. G., Jr.; Spencer, D. J. E.; Tolman, W. B. *Inorg. Chem.* **2001**, *40*, 6097.
(30) From a search of the Cambridge Crystallographic Database, CSDversion 5.26 (November 2004). Values for Cu(II) systems are based on 92 structures and 217 Cu−S distances; for Cu(I) systems, they are based on 109 structures and 344 Cu−S distances.

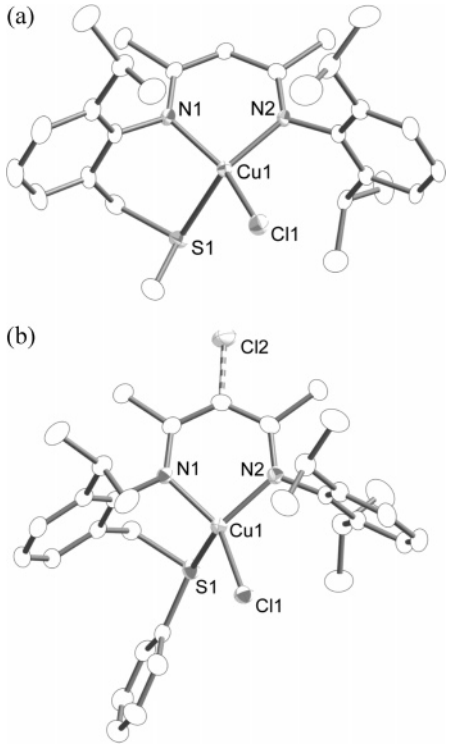

Figure 3. Representations of the X-ray structures of (a) $L^{iPr,SMe}CuCl$ and (b) $L^{iPr,SPh}CuCl$. All atoms are shown as 50% thermal ellipsoids, with hydrogen atoms omitted for clarity. Selected interatomic distances (Å) and angles (deg) are as follows: (a) Cu1−N1, 1.906(3); Cu1−N2, 1.956(3); Cu1−Cl1, 2.2177(11); Cu1−S1, 2.3793(11); N1−Cu1−N2, 94.26(13); N1−Cu1−S1, 92.67(10); N2−Cu1−Cl1, 105.29(9); S1−Cu1−Cl1, 95.78(4). (b) Cu1−N1, 1.888(2); Cu1−N2, 1.934(2); Cu1−Cl1, 2.1846(9); Cu1−S1, 2.5941(9); N1−Cu1−N2, 94.42(10); N1−Cu1−S1, 89.48(8); N2−Cu1−Cl1, 108.59(8); S1−Cu1−Cl1, 100.27(3).

CuCl bear some resemblance to that in the thiolate−thioether model of oxidized type 1 "blue" copper centers, $Me_2L^{iPr2}Cu(SCPh_2CH_2SMe)$, where the Cu(II)−S(thioether) distance is 2.403(1) Å (Figure S2).[31]

In the structures of both complexes, unexpected electron density was found near the ligand backbone carbon C3 that was too significant to be considered residual. Given the distance from C3 (1.685(11) Å for X = Me and 1.708(3) Å for X = Ph), the density was best modeled as a chlorine atom at partial occupancy. This compositional disorder refined to a 90:10 ratio of hydrogen:chlorine occupancy for R = Me and a 53:47 ratio for X = Ph (Figure 3b). Corroborating these assignments, high-resolution mass spectra of the complexes showed peaks attributable to the parent ions both for $Me_2L^{iPr,SX}CuCl$ and for the backbone-chlorinated versions (see Experimental Section). The source of the partial chlorination of the ligand backbone is likely the $CuCl_2$·0.8THF reagent. However, the mechanism for the chlorination is unknown, and such a reaction has not been observed in previously reported β-diketiminate Cu(II)−chloride complexes.[29] Despite the compositional disorder at C3, there is no further disorder in the X-ray structures and the R1 values of 0.0566 for X = Me and 0.0472 for X = Ph indicate good quality crystal data. Most importantly, there is no disorder in the thioether arm, and thus in the solid state, intramolecular binding of the thioether sulfur to the Cu(II) center occurs in both the non-chlorinated and the chlorinated species.

The UV−vis spectra of $Me_2L^{iPr,SX}CuCl$ in CH_2Cl_2 resemble that reported previously for $Me_2L^{iPr2}CuCl$,[28] clearly indicating that the complexes exist as monomers in solution, yet suggesting that the thioether group dissociates to yield 3-coordinate species (Figure S3). This latter conclusion remains tentative, however, in view of the subtle differences between the spectra (cf., the extinctions and widths of the near-IR feature) and the potential complications from the presence of backbone-chlorinated byproducts.

Synthesis and Characterization of Cu(I) Complexes. Complexes of $(Me_2L^{iPr,SX})^-$ with Cu(I) were prepared either by mixing $Li(Me_2L^{iPr,SMe})$ with CuCl or by reaction of $Me_2L^{iPr,SPh}H$ with $(Me_3SiCH_2Cu)_4$[32] in THF (Scheme 1). The products correspond to the empirical formula $Me_2L^{iPr,SX}Cu$ according to analytical data (CHN analysis, high-resolution mass spectrometry). In the case of the complex with $(Me_2L^{iPr,SMe})^-$, addition of 1 equiv of PPh_3 yielded a monomeric adduct, $Me_2L^{iPr,SMe}Cu(PPh_3)$. This adduct and its precursor Cu(I) complex were characterized by X-ray crystallography (Figure 4).

In contrast to the monomeric structures observed for the Cu(II) complexes $Me_2L^{iPr,SX}CuCl$, the Cu(I) complex of $(Me_2L^{iPr,SMe})^-$ crystallizes as a tetramer, in which only one-half of the molecule is unique, and the other half is grown by symmetry through an inversion center. Rather than binding to the copper center to which its N-donors are bound (i.e., in intramolecular fashion), the thioether arm of each ligand binds to the copper center of the adjacent $Me_2L^{iPr,SMe}Cu$ fragment.[33] The lack of any intramolecular Cu−S interaction is confirmed by distances from the copper centers to the thioether sulfurs of the same ligand that includes its N-donors that are all greater than 3.77 Å. The intermolecular Cu(I)−S distances of ∼2.16 Å are considerably shorter than the Cu−S distances observed in the Cu(II)−chloride complexes discussed above (∼2.38 and 2.59 Å), a typical phenomenon[27b,34,35] that may be rationalized by hard−soft acid−base considerations (favorable interaction of the soft thioether sulfur donor and the low-valent d^{10} Cu(I) center). In a survey of the Cambridge Crystallographic Structural Data Centre for Cu−S bond distances in Cu(I)−thioether complexes, the average bond distance is 2.31 Å over a range of 2.19−2.88 Å, as compared to the average Cu−S distance of 2.41 Å for Cu(II)−thioether complexes.[30] Thus, the Cu(I)−thioether bond distances here lie toward the short end of the range for Cu(I) complexes, indicating relatively strong binding of the thioether arm. Nonetheless, upon reaction of $[Me_2L^{iPr,SMe}Cu]_4$ with PPh_3, the thioether arm is displaced to yield a monomeric 3-coordinate complex, $Me_2L^{iPr,SMe}Cu(PPh_3)$ (Figure 4b). The Cu−N and Cu−P bond distances in this compound are similar to those observed for the previously reported complex $Me_2L^{iPr2}Cu(PPh_3)$.[36] Finally, although the crystal structure of

(31) Holland, P. L.; Tolman, W. B. *J. Am. Chem. Soc.* **2000**, *122*, 6331.

(32) (a) Lappert, M. F.; Pearce, R. *Chem. Commun.* **1973**, 24-2. (b) Jarvis, J. A.; Kilbourn, B. T.; Pearce, R.; Lappert, M. F. *Chem. Commun.* **1973**, 475. (c) Jarvis, J. A.; Pearce, R.; Lappert, M. F. *J. Chem. Soc., Dalton Trans.* **1977**, 999.

(33) Similar "intermolecular" coordination of thioether groups in oligomeric Cu(I) complexes has been reported. See: (a) Yim, H. W.; Tran, L. M.; Pullen, E. E.; Rabinovich, D. *Inorg. Chem.* **1999**, *38*, 6234. (b) Tanaka, R.; Yano, T.; Nishioka, T.; Nakajo, K.; Breedlove, B. K.; Kimura, K.; Kinoshita, I.; Isobe, K. *Chem. Commun.* **2002**, 1686.

(34) Ambundo, E. A.; Deydier, M.-V.; Grall, A. J.; Aguera-Vega, N.; Dressel, L. T.; Cooper, T. H.; Heeg, M. J.; Ochrymowycz, L. A.; Rorabacher, D. B. *Inorg. Chem.* **1999**, *38*, 4233.

(35) Ohta, T.; Tachiyama, T.; Yoshizawa, K.; Yamabe, T.; Uchida, T.; Kitagawa, T. *Inorg. Chem.* **2000**, *39*, 4358.

(36) Reynolds, A. M.; Lewis, E. A.; Aboelella, N. W.; Tolman, W. B. *Chem. Commun.* **2005**, 2014.

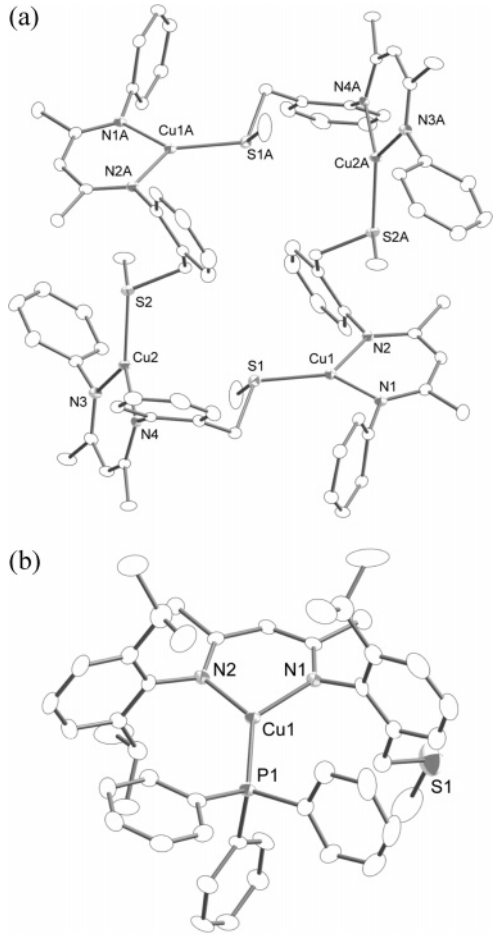

Figure 4. Representations of the X-ray structures of (a) $[Me_2L^{iPr,SMe}Cu]_4$ and (b) $Me_2L^{iPr,SMe}Cu(PPh_3)$. All atoms are shown as 50% thermal ellipsoids, with hydrogen atoms omitted for clarity. The isopropyl groups in $[Me_2L^{iPr,SMe}Cu]_4$ also are omitted to facilitate visualization of the structure. Selected interatomic distances (Å) and angles (deg) are as follows: (a) Cu1−N1, 1.928(3); Cu1−N2, 1.953(3); Cu1−S1, 2.1637(9); Cu2−N3, 1.963(3); Cu2−N4, 1.935(2); Cu2−S2, 2.1581(8); N1−Cu1−N2, 98.90(11); N1−Cu1−S1, 132.19(8); N2−Cu1−S1, 128.88(8); N3−Cu2−N4, 99.05(11); N3−Cu2−S2, 123.72(8); N4−Cu2−S2, 136.41(8). (b) Cu1−N1, 1.956(3); Cu1−N2, 1.950(3); Cu1−P1, 2.1687(11); N1−Cu1−N2, 98.52(14); N1−Cu1−P1, 128.28(11); N2−Cu1−P1, 132.66(10).

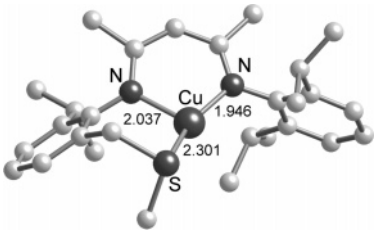

Figure 5. Minimum energy structure for $Me_2L^{iPr,SMe}Cu$ determined from DFT calculations, with metal−ligand bond distances indicated and hydrogen atoms omitted for clarity.

$Me_2L^{iPr,SPh}Cu$ was not obtained, given its spectroscopic similarities to $Me_2L^{iPr,SMe}Cu$ (vide infra), it is likely that it also displays a similar multinuclear topology in the solid state.

In addition to X-ray crystallography, DFT calculations were performed to determine the minimum energy structure for $Me_2L^{iPr,SMe}Cu$ (Figure 5). Although the calculations do not address the possibility of higher nuclearity species, they predict that the preferred structure for a monomeric complex includes the thioether bound to the copper with a Cu−S distance of 2.301 Å. Increasing the Cu−S distance leads to geometries with steadily increasing electronic energies (Figure S4). At a Cu−S distance of 3.0 Å, where the thioether may be considered dissociated from Cu, the electronic energy has risen by 7.2 kcal/mol. Increases in the Cu−S distance also correlate with decreasing Wiberg Cu−S bond indices (Figure S5).[37,38] Thus, although the X-ray crystal structures reveal multinuclear species for the Cu(I) complexes in the solid state, the DFT calculations suggest that if a mononuclear species were accessible (e.g., in solution), thioether binding would be favored.

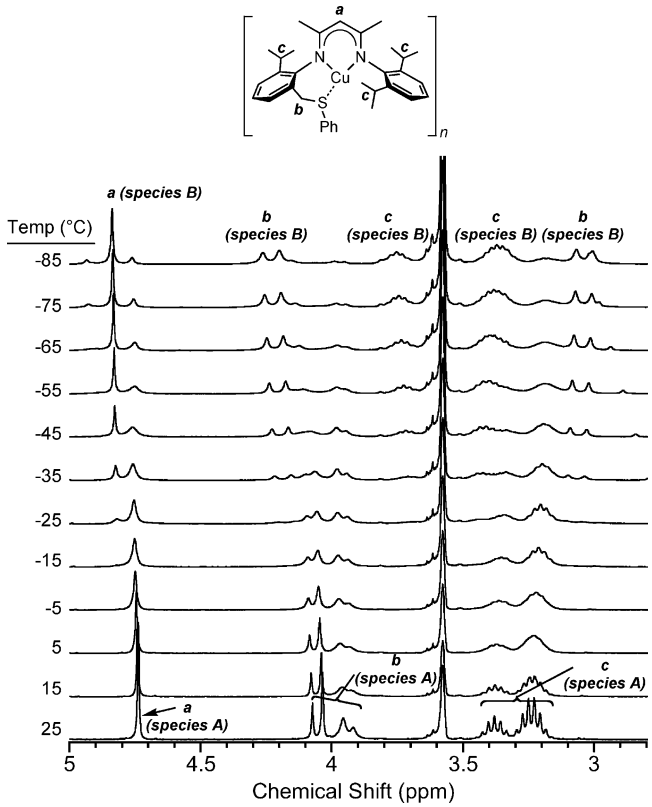

Figure 6. Selected region of the variable-temperature ^1H NMR spectra of $Me_2L^{iPr,SPh}Cu$ (THF-d_8, 300 MHz) with assignments indicated (see text).

To probe the structures of the Cu(I) complexes in solution, ^1H NMR spectra were recorded in different solvents (C_6D_6 or THF-d_8) and at various temperatures. The VT-NMR spectra recorded between 25 and −85 °C in THF-d_8 for $Me_2L^{iPr,SX}Cu$ (X = Me or Ph) are similar (Figures S6 and S7). Particularly revealing portions of the spectra for $Me_2L^{iPr,SPh}Cu$ are shown with assignments in Figure 6. At 25 °C, a singlet ("a") is observed for the central −C*H* on the ligand backbone at 4.74 ppm that suggests the presence of a single species at this temperature. However, the pattern for the diastereotopic thioether methylene −CH_2 protons at 3.9−4.1 ppm ("b") deviates from that expected for an AB or AX system, insofar as the upfield peaks are broadened considerably more than the downfield set. We assign this spectrum to a single molecule (species A) that participates in a fluxional process ("high T process") that affects one of the diastereotopic protons more than the other, such that at 25 °C they exhibit different line widths. Upon cooling, the intensity

(37) Glendening, E. D.; Badenhoop, J. K.; Reed, A. E.; Carpenter, J. E.; Bohmann, J. A.; Morales, C. M.; Weinhold, F. (Theoretical Chemistry Institute, University of Wisconsin, Madison, WI, 2001); http://www.chem.wisc.edu/~nbo5.
(38) Wiberg, K. B. *Tetrahedron* **1968**, *24*, 1083.

Table 1. Selected Spectroscopic Properties of Cu(I) Complexes and Cu/O_2 Intermediates[a]

complex	UV–vis: λ_{max}, nm (ϵ, $M^{-1}\,cm^{-1}$)	Raman (cm^{-1})[b]	ref
$Me_2L^{iPr,SMe}Cu(I)$	255 (sh, 16 700), 280 (sh, 13 600), 357 (18 200), 382 (16 400)		this work
$Me_2L^{iPr,SPh}Cu(I)$	255 (sh, 15 600), 275 (sh, 13 300), 360 (16 300), 382 (15 200)		this work
$Me_2L^{iPr,SMe}CuO_2$	332 (26 700), 395 (sh, 2000), 610 (200)	990/971[c] 991/969 (925)[d]	this work
$Me_2L^{iPr,SMe}CuO_2$	331 (28 500), 395 (sh, 2000), 595 (200)	994/971[c] 994/970 (925)[d]	this work
$Me_2L^{iPr2}CuO_2$ (**2a**, R = Me)	385 (~2400), 600 (200)	968 (917)[e]	19a
$tBu_2L^{iPr2}CuO_2$ (**2a**, R = *t*Bu)	424 (2000), 638 (200)	961 (912)[e]	19b
2b	390 (sh, 7600), 440 (10 300), 453 (11 300), 650 (200)	974 (908)[e]	19d
$[(Me_2L^{iPr,SMe}Cu)_2(\mu\text{-}O)_2]$	448 (~11 000)[f]	592 (567)[g]	this work
$[(Me_2L^{iPr,SPh}Cu)_2(\mu\text{-}O)_2]$	443 (~6000)[f]	593 (567)[g]	this work
$[(Me_2L^{Et2}Cu)_2(\mu\text{-}O)_2]$	426 (10 000)[f]	604 (577)[g]	22

[a] Except as noted, all UV−vis and resonance Raman spectra were measured in THF, with extinction coefficients reported per copper. UV−vis spectra were obtained at −80 °C, and resonance Raman spectra were obtained at −196 °C. [b] Reported as Raman shifts for samples prepared with $^{16}O_2$ ($^{18}O_2$). [c] ν(O−O), THF, λ_{ex} = 406.7 nm, data for compound prepared from $^{18}O_2$ unavailable due to spectral overlap with a solvent peak. [d] ν(O−O), CH_2Cl_2, λ_{ex} = 406.7 nm. [e] ν(O−O), acetone, λ_{ex} = 413.1 nm. [f] Extinction coefficient reported per bis(μ-oxo)dicopper complex. [g] $\nu(Cu_2O_2)$, λ_{ex} = 457.9 nm.

of the central −C*H* peak at 4.74 ppm decreases while a new −C*H* singlet appears at 4.83 ppm ("a"). Concurrently, the peaks due to the thioether methylene $-CH_2$ protons centered at 4 ppm decrease in intensity, while two new doublets for these protons grow in at vastly different chemical shifts (4.23 and 3.03 ppm, J = 18.6 Hz, "b"). The multiplets attributed to the isopropyl substituent methine −C*H* protons (3.2−3.4 ppm, "c") also change upon cooling, but to multiple broad signals that precluded definitive assignment.

We interpret the changes in the ^{1}H NMR spectrum upon cooling to indicate that the species present at higher temperature (species A) equilibrates with a second species (B) that has a structure sufficiently different from that of A to effect a major change in the chemical shift difference between the diastereotopic thioether methylene protons.[39] Within the rubric of this hypothesis, we estimated equilibrium constants (K_{eq} = [B]/[A]) at each temperature by integrating the singlets for the ligand backbone −C*H* protons and obtained thermodynamic parameters from a plot of ln(K_{eq}) versus 1/T (Figure S8): $\Delta H° = -18.3(5)$ kJ mol^{-1} and $\Delta S° = -82(4)$ J mol^{-1} K^{-1}. Although definitive structural assignments for species A and B are not possible to obtain with the available data, the large chemical shift difference between the thioether methylene signals in species B and the significantly negative entropy value for its equilibration with species A are consistent with B being an oligomeric species with intermolecular thioether coordination akin to that of $[Me_2L^{iPr,SMe}Cu]_4$ identified in the crystalline state. Accordingly, we postulate that species A is a monomeric species such as that defined by theory (Figure 5) and that the "high T process" discussed above entails rapid coordination and decoordination of the thioether arm, perhaps with involvement of THF solvent. Notwithstanding the necessarily tentative nature of these particular structural hypotheses, it is clear that the Cu(I) complexes of $(Me_2L^{iPr,SX})^-$ undergo fluxional processes in solution that involve significant changes in the chemical environment of the thioether arm. These changes are most consistent with alterations in the mode of copper coordination by the thioether group.

Oxygenation Reactions of Cu(I) Complexes: 1:1 Cu/O_2 Adducts. The reactions of $Me_2L^{iPr,SX}Cu$ with dioxygen at −80 °C in THF or toluene lead to significant changes in the electronic absorption spectra (Figure 7, for X = Me). Upon oxygenation, the yellow Cu(I) solution becomes bright green, a shift in the high energy $\pi-\pi^*$ transitions occurs, and a very slight shoulder appears at ~395 nm for both complexes, along with a less intense broad feature at ~600 nm. The oxygenated solutions are EPR silent. The UV−vis absorption features degrade upon warming the solutions to room temperature, indicating the formation of thermally unstable intermediates. The similarity of these spectroscopic features to those observed for the previously reported systems $R_2L^{iPr2}CuO_2$ (R = Me or *t*Bu, Table 1)[19b] suggests that related 1:1 Cu/O_2 adducts are formed in the thioether-appended ligand system.

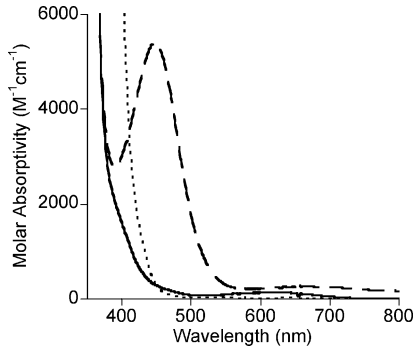

Figure 7. UV−vis spectra in THF at −80 °C of $Me_2L^{iPr,SMe}Cu$ (dotted line), the product of its oxygenation (solid line), and the species resulting after purging the oxygenation product solution with argon (dashed line).

Resonance Raman spectroscopy was used to further characterize the oxygenation intermediates. Initial data for the species prepared with $^{16}O_2$ were acquired using THF solutions (λ_{ex} = 406.7 nm, Table 1), but a peak derived from solvent (929 cm^{-1}) obscured the key region of the spectrum in samples prepared using $^{18}O_2$. To observe Raman features for both $^{16}O_2$- and $^{18}O_2$-derived samples, we therefore examined the low-temperature oxygenations of $Me_2L^{iPr,SX}Cu$ in CH_2Cl_2. At room temperature, solutions of the Cu(I) complexes in CH_2Cl_2 showed signs of decay within minutes, presumably due to a chlorination reaction similar to that which has been described for other Cu(I) compounds.[40] Nevertheless, by working quickly the oxygenation

(39) The UV−vis spectra of $Me_2L^{iPr,SR}Cu$ in THF also change upon cooling (data not shown), consistent with the hypothesis of equilibria between multiple species in solution. These data do not allow structural assignments to be determined, however.

(40) (a) Osako, T.; Karlin, K. D.; Itoh, S. *Inorg. Chem.* **2005**, *44*, 410. (b) Lucchese, B.; Humphreys, K. J.; Lee, D.-H.; Incarvito, C. D.; Sommer, R. D.; Rheingold, A. L.; Karlin, K. D. *Inorg. Chem.* **2004**, *43*, 5987. (c) Jacobson, R. R.; Tyeklár, Z.; Karlin, K. D. *Inorg. Chim. Acta* **1991**, *181*, 111.

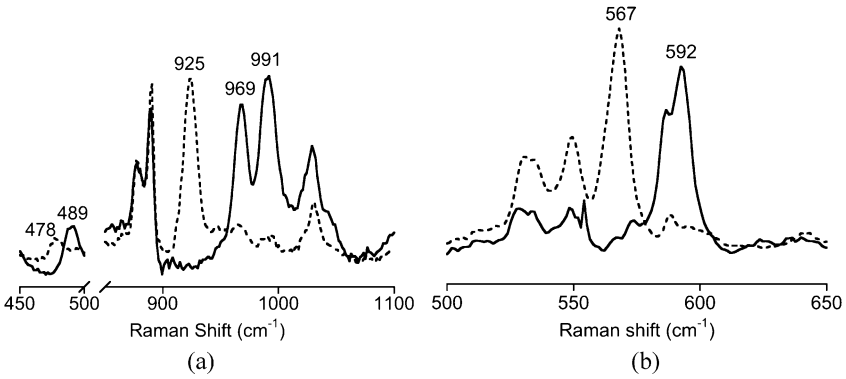

Figure 8. Resonance Raman spectra with O-isotope sensitive peaks labeled of frozen solutions (77 K) of (a) the product of the reaction of $Me_2L^{iPr,SMe}Cu$ in CH_2Cl_2 with $^{16}O_2$ (solid line) or $^{18}O_2$ (dashed line), using $\lambda_{ex} = 406.7$ nm, and (b) the species resulting from argon purging of the oxygenation product $Me_2L^{iPr,SMe}CuO_2$ obtained using $^{16}O_2$ (solid line) or $^{18}O_2$ (dashed line), using $\lambda_{ex} = 457.9$ nm.

reactions could be performed without significant decomposition of the Cu(I) precursors. The UV−vis and resonance Raman data in CH_2Cl_2 were similar to those obtained in THF, with the added benefit of being able to observe new peaks in the spectrum acquired on the samples prepared with $^{18}O_2$. The data are shown in Figures 8a (X = Me) and S9 (X = Ph), with all oxygen-isotope sensitive features listed in Table 1. For both complexes, two peaks at ∼970 and ∼992 cm^{-1} shift to a single peak at 925 cm^{-1} upon ^{18}O substitution. These peaks are in the same region as the O−O stretching vibration identified in **2**,[19] suggesting an analogous assignment. In addition, weak features at 489 cm^{-1} (X = Me) or 494 cm^{-1} (X = Ph) are also ^{18}O-isotope sensitive ($\Delta^{18}O \approx 14$ cm^{-1}); these are consistent with Cu−O vibrations. We hypothesize that the two O-isotope-sensitive bands in the $^{16}O_2$ spectrum between 970 and 992 cm^{-1} are Fermi doublets arising from coupling of the O−O stretch to a harmonic of the low-frequency feature.[41] In support of this notion, the second overtone (2ν) of the low-frequency feature is 978 cm^{-1} (X = Me) or 988 cm^{-1} (X = Ph), in close agreement with the average of the two observed peaks, 980 cm^{-1} (X = Me) or 982 cm^{-1} (X = Ph). In line with the hypothesis of a Fermi doublet, the coupling disappears in the $^{18}O_2$ spectrum because in this case 2ν is ∼958 cm^{-1}, far from the $\nu(^{18}O-^{18}O)$ at 925 cm^{-1}. Finally, on the basis of the observed Raman shift for the $^{18}O-^{18}O$ stretch (925 cm^{-1}), the calculated $^{16}O-^{16}O$ stretch should appear at 981 cm^{-1} ($\Delta^{18}O_2$(calc) = 56 cm^{-1}), which closely matches the average of the doublets. Taken together, the data are most consistent with a $\nu(^{16}O-^{16}O)$ for both complexes at ∼981 cm^{-1} that appears as a doublet due to Fermi coupling to the second overtone of the ν(Cu−^{16}O) at ∼493 cm^{-1}.

The similarity of the UV−vis features and ν(O−O) values for the oxygenation products of $Me_2L^{iPr,SX}Cu$ to those of **2a** and **2b** (Table 1) comprises strong evidence that they exhibit analogous side-on (η^2) O_2 coordination. Further insight was provided by DFT/CASPT2 calculations, which concluded the side-on singlet Cu−O_2 adduct to be most stable among the singlet and triplet end-on and side-on possibilities for $Me_2L^{iPr,SMe}CuO_2$ (Table 2). The triplet cases are distinctly higher in energy than the corresponding singlets and will not be discussed any further here. For the η^2 adduct, the Cu−S bond present in

Table 2. Computed DFT/CASPT2 Free Energies (kcal/mol) for $Me_2L^{iPr,SMe}CuO_2$ Relative to the η^2 Singlet Case

	gas phase 25 °C	THF −80 °C
η^1 singlet	7.0	6.0
η^1 triplet	18.4	19.8
η^2 singlet	0.0	0.0
η^2 triplet	15.0	16.4

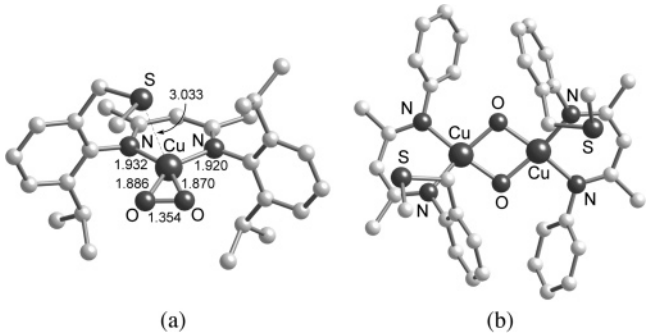

Figure 9. Minimum energy structures calculated using DFT of (a) $Me_2L^{iPr,SMe}CuO_2$ and (b) $[(Me_2L^{H,SMe}Cu)_2(\mu\text{-}O)_2]$ (hydrogen atoms omitted for clarity, with distances in Å). Selected distances for the structure in (b) are: Cu−Cu, 2.926 Å; O−O, 2.301 Å; Cu−O, 1.86 Å; Cu−S, 4.84 Å.

$Me_2L^{iPr,SMe}Cu$ has effectively dissociated and the Cu−S distance has increased by 0.7 Å to 3.033 Å (Figure 9a). Further increasing this interatomic distance leads to a steady but minimal increase (<1 kcal/mol) in energy (Figure S10). Decreasing the Cu−S separation back to that observed in $Me_2L^{iPr,SMe}Cu$ leads to a much sharper increase in energy; in particular, at 2.30 Å, the electronic energy is increased by 11 kcal/mol. This result can be contrasted with the optimized structure for the end-on adduct, in which the thioether remains ligated to Cu at a distance of 2.550 Å (Figure S11). A structure similar to the side-on case in which the Cu−S bond is severed occurs at a local minimum with an electronic energy higher by 1.3 kcal/mol and a Cu−S distance of ∼2.95 Å (Figure S12). Comparison of the end-on and side-on structures reveals that if one were to move from the former to the latter ($\eta^1 \rightarrow \eta^2$ isomerization) a steric clash between the thioether group and the oxygen atom distal from the Cu center develops, which rationalizes the longer Cu−S distance in the side-on case. In addition, the significant Cu(III)−peroxo character (vide infra) of the side-on adduct would disfavor axial ligation of the thioether due to the bonding preferences of the d^8 metal center.

(41) Czernuszewicz, R. S.; Spiro, T. G. In *Inorganic Electronic Structure and Spectroscopy Vol. 1, Methodology*; Solomon, E. I., Lever, A. B. P., Eds.; John Wiley & Sons: New York, 1999; pp 353−441.

Table 3. Computed and Experimentally Determined ν(O−O) and ν(Cu−O) (cm^{-1}) for the Singlet States of $Me_2L^{iPr,SMe}CuO_2$

	vibration	$^{16}O-^{16}O$	$\Delta(^{18}O-^{16}O)^a$	$\Delta(^{16}O-^{18}O)^a$	$\Delta(^{18}O-^{18}O)$
η^1 computed	O−O	1194.6	36.2	35.9	70.7
η^2 computed	O−O	1055.7	29.3	29.2	59.9
experimental	O−O	981	n/a	n/a	56
η^1 computed	Cu−O	437.2	19	16.8	20.0
η^2 computed	Cu−O	461.4	4.7	4.6	13.5
experimental	Cu−O	489	n/a	n/a	14

[a] The first O is the oxygen having the shortest distance to Cu.

Comparison of the computed and experimental O−O and Cu−O stretch frequencies in the 1:1 adducts (Table 3) shows that the calculated side-on structure is most consistent with the experimental $\nu(^{16}O_2)$ and $\Delta\nu(^{18}O_2)$ data. Although the calculated ν(O−O) values of the mixed-label isotopomers (i.e., $^{16}O-^{18}O$ vs $^{18}O-^{16}O$) are nearly identical in the η^2 structure, as would be expected with a symmetrically coordinated O_2 ligand, the results are similar in the asymmetrically bound η^1 case. These findings are in agreement with previous work that has shown that using isotopomeric splitting to differentiate end-on and side-on coordination is problematic.[42,43]

As has been concluded for the 1:1 adducts **2a** and **2b**,[19c,d] the side-on $Me_2L^{iPr,SMe}CuO_2$ structure lies intermediate along the continuum[20] between the Cu(II)−superoxo and Cu(III)−peroxo extremes, although somewhat closer to the peroxo limit. This conclusion is based upon a collective assessment of the geometric, vibrational, and electronic data for the structure. The O−O bond length of 1.354 Å is nearly the average of the ∼1.3 and ∼1.4 Å distances associated with superoxide and peroxide, respectively. The vibrational frequencies characteristic of superoxo ligands (1075−1200 cm^{-1}) and peroxo ligands (790−930 cm^{-1}) also frame the computed and experimental ν(O−O) values. Occupation numbers from the CAS calculation for the two orbitals that most contribute to the multideterminantal character of the side-on adduct (Figure S13) are 1.64 and 0.39 and imply that the structure lies approximately two thirds of the way toward Cu(III)−peroxo.[44]

The free energy change for the reaction of $Me_2L^{iPr,SMe}Cu$ with dioxygen to form the singlet side-on $Me_2L^{iPr,SMe}CuO_2$ is −20.5 kcal/mol at the experimental conditions of THF solvent and −80 °C and assuming standard 1 M concentrations. When basis set superposition error (BSSE) is accounted for via counterpoise calculations, ΔG increases by 5.5 kcal/mol to −15.0 kcal/mol. The oxygenation reaction is thus predicted to be exergonic. At the initial experimental reactant concentrations (0.2−10 mM), the reaction proceeds to virtual completion; at the O_2 binding equilibrium, the amount of free Cu(I) complex relative to $Me_2L^{iPr,SX}CuO_2$ is predicted to be extremely small (0.03−0.23 ppm).

Overall, the side-on theoretical structure for $Me_2L^{iPr,SMe}CuO_2$ bears much similarity to the analogous O_2 adduct **2a**.[19a−c] Coordination of dioxygen to Cu is nearly symmetric in both systems, which may be expected considering the Cu ligation is essentially identical once the Cu−S ligation is removed. The slight asymmetry that is present with regard to Cu−O distances in $Me_2L^{iPr,SMe}CuO_2$ can be attributed to the steric effect of the thioether appendage, which causes the proximal Cu−O bond to be 0.016 Å longer than the distal counterpart (Figure 9a). On the other hand, the η^1 $Me_2L^{iPr,SMe}CuO_2$ isomer is ∼3 kcal/mol less stable versus the η^2 isomer as compared to the corresponding difference in **2a**. This occurs despite the presence of the Cu−S bond in the η^1 $Me_2L^{iPr,SMe}CuO_2$ isomer, which confers 1.3 kcal/mol of stability to this structure (cf., Figures S11, S12). Instead, the difference is attributable to the spatial proximity of the thioether to the dioxygen moiety, which forces O_2 to bind at an angle (i.e., the difference in N−Cu−O bond angles is 52.4°), decreasing the favorable orbital overlap between the Cu d and O_2 π^* orbitals in the Cu/O_2 bonding molecular orbital (Figure S14).

Reactivity of the 1:1 Cu/O_2 Adducts. (a) Argon Purging. While the above evidence suggests that the thioether substituent does not appreciably affect the electronic structure and O_2 coordination mode relative to the complexes **2a** and **2b**, other evidence indicates that it does influence the thermodynamics of dioxygen binding. Whereas the formation of **2a** and **2b** is irreversible, such that free dioxygen may be removed from solutions of these complexes without degradation, prolonged and vigorous bubbling of argon through O_2-saturated THF or toluene solutions of $Me_2L^{iPr,SX}CuO_2$ at −80 °C resulted in a color change from bright green to yellow-brown and development of an intense UV−vis absorption feature at ∼445 nm (Figure 7). The rate of formation of the yellow-brown species is highly dependent on the rate of argon bubbling through the solution (faster rate with more rapid bubbling); conversion was not observed if the bubbling was gentle or performed for only a short time. The ∼445 nm feature decays upon warming the solutions to room temperature, indicating that it arises from a thermally unstable species, and closely resembles a signature absorption band of the bis(μ-oxo)dicopper(III) core. Diagnostic features for this core were also observed in resonance Raman spectra (THF, λ_{ex} = 457.9 nm, 77 K) obtained for samples prepared with $^{16}O_2$ or $^{18}O_2$ (Figures 8b (X = Me) and S15 (X = Ph)). For example, for X = Me, we observed a band at 592 cm^{-1} with $\Delta^{18}O$ = 25 cm^{-1} (Table 1), which are typical values for the symmetric Cu_2O_2 core vibration.[4a,45] Thus, on the basis of the available spectroscopic evidence, we propose that argon purging results in the formation of [$(Me_2L^{iPr,SX}Cu)_2(\mu$-$O)_2$].

Theoretical calculations corroborate generation of [$(Me_2L^{iPr,SMe}$-$Cu)_2(\mu$-$O)_2$] rather than its μ-η^2:η^2-peroxo isomer and provide structural and energetic insights. Using a slightly truncated model system in which the isopropyl groups were changed to hydrogen atoms for computational expediency, calculations were performed with the BLYP[46] density functional using both restricted and unrestricted methodologies. Singlet geometries for both [$(Me_2L^{H,SMe}Cu)_2(\mu$-$O)_2$] and [$(Me_2L^{H,SMe}Cu)_2(\mu$-η^2:η^2-$O_2)$] were optimized using the DZP basis and final energies were determined using the TZP basis[47] (see computational

(42) Kinsinger, C. R.; Gherman, B. F.; Gagliardi, L.; Cramer, C. J. *J. Biol. Inorg. Chem.* **2005**, *10*, 778−789.
(43) Schatz, M.; Raab, V.; Foxon, S. P.; Brehm, G.; Schneider, S.; Reiher, M.; Holthausen, M. C.; Sundermeyer, J.; Schindler, S. *Angew. Chem., Int. Ed.* **2004**, *43*, 4360.
(44) Occupation numbers of 1.00 and 1.00 correspond to a pure Cu(II)−superoxo mesomer, while 2.00 and 0.00 correspond to a pure Cu(III)−peroxo mesomer. Occupation numbers between these two extremes provide a quantitative measure of the point at which structures lie along the continuum between these mesomers.
(45) (a) Mahapatra, S.; Halfen, J. A.; Wilkinson, E. C.; Pan, G.; Wang, X.; Young, V. G., Jr.; Cramer, C. J.; Que, L., Jr.; Tolman, W. B. *J. Am. Chem. Soc.* **1996**, *118*, 11555. (b) Henson, M. J.; Mukherjee, P.; Root, D. E.; Stack, T. D. P.; Solomon, E. I. *J. Am. Chem. Soc.* **1999**, *121*, 10332.
(46) (a) Johnson, B. G.; Gill, P. M. W.; Pople, J. A. *J. Chem. Phys.* **1993**, *98*, 5612. (b) Becke, A. D. *J. Chem. Phys.* **1993**, *98*, 1372. (c) Lee, C. T.; Yang, W. T.; Parr, R. G. *Phys. Rev. B* **1988**, *37*, 785.
(47) Siegbahn, P. E. M. *J. Biol. Inorg. Chem.* **2003**, *8*, 577.

methods section). Solvation energies were calculated as well, but vibrational frequency calculations proved prohibitively expensive due to the ~90-atom model size. Unrestricted calculations on both the bis(μ-oxo) and the μ-η^2:η^2-peroxo isomers converged to the restricted solution. The electronic energy including solvation at −80 °C in THF (E_{solv}) was 9.3 kcal/mol lower for the bis(μ-oxo)dicopper(III) geometry (Figure 9b).[48] This energy difference changes to 8.0 kcal/mol in the gas phase, indicating that the bis(μ-oxo) geometry is better solvated by 1.3 kcal/mol. The effect is less than was seen in comparable calculations on $\{[(NH_3)_3Cu]_2(\mu\text{-}O)_2\}^{2+}$ and $\{[(NH_3)_3Cu]_2(\mu\text{-}\eta^2\text{:}\eta^2\text{-}O_2)\}^{2+}$,[49] likely due to the steric bulk of the methyl and phenyl groups partially screening the larger core charges in the bis(μ-oxo) versus peroxo isomers. The geometry for the triplet state of the $[(Me_2L^{H,SMe}Cu)_2(\mu\text{-}\eta^2\text{:}\eta^2\text{-}O_2)]$ peroxo isomer has a butterflied core, in contrast to the planar core of the singlet state (Figure S16), and was computed to be 5.3 kcal/mol higher in energy than the corresponding singlet and 14.6 kcal/mol less stable than the bis(μ-oxo) form.

The optimized $[(Me_2L^{H,SMe}Cu)_2(\mu\text{-}O)_2]$ structure shows no copper−sulfur interactions, with the interatomic Cu−S distances of 4.84 Å and the Cu centers having distorted square planar coordination geometries. Orientations of the two $(Me_2L^{H,SMe})^-$ ligands were explored in which the two thioether appendages were either anti or syn relative to the Cu_2O_2 plane, with the latter leading to structures 1−2 kcal/mol lower in energy. The small energy difference is unsurprising given the lack of Cu−S bonding and the large distance (~4.3 Å) between the thioether appendages even when they are in the syn configuration.

To determine the energy of formation of $[(Me_2L^{H,SMe}Cu)_2(\mu\text{-}O)_2]$ from $Me_2L^{H,SMe}CuO_2$ and $Me_2L^{H,SMe}Cu$, geometry optimization followed by single-point energy calculations for the 1:1 adduct and Cu(I) complex were carried out at the BLYP/DZP and BLYP/TZP levels of theory, respectively. No CASPT2 correction was made to the energy computed for $Me_2L^{H,SMe}CuO_2$. Rather, it is presumed that the error in this energy is approximately equal to the error in the BLYP energy for the bis(μ-oxo) energy; that is, that BLYP improperly destabilizes both to the same degree. This error cancels out in computing the energy of reaction, which was then determined to be −20.8 kcal/mol at 193 K in THF (assuming standard state concentrations of reactants). If the ΔS of this bimolecular reaction is approximated to be on the order of −40 cal/mol·K (e.g., on the basis of comparison with computed ΔS of the oxygenation reaction),[50] the free energy of reaction is estimated to be −13 kcal/mol. The reaction to form $[(Me_2L^{H,SMe}Cu)_2(\mu\text{-}O)_2]$ is thus thermodynamically favorable, consistent with the experimental results.

Scheme 2

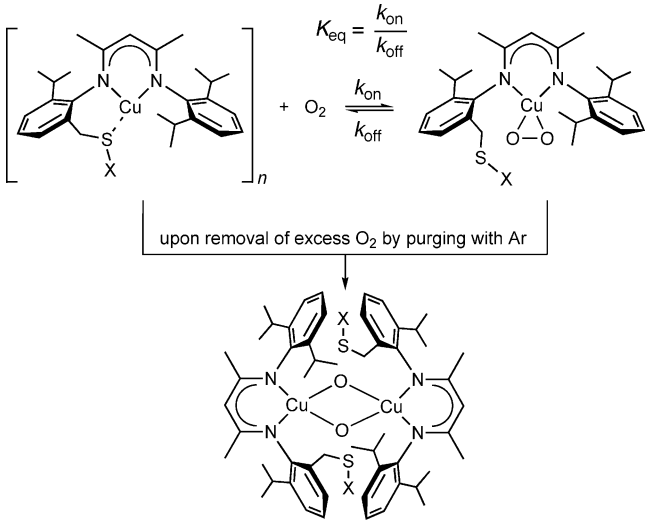

To rationalize the experimentally observed formation of $[(Me_2L^{iPr,SX}Cu)_2(\mu\text{-}O)_2]$ from $Me_2L^{iPr,SX}CuO_2$, we propose that (i) argon purging promotes O_2 loss from $Me_2L^{iPr,SX}CuO_2$ to yield a Cu(I) species, which (ii) is trapped by unreacted $Me_2L^{iPr,SX}CuO_2$ (Scheme 2). Both the absence of an observable amount of bis(μ-oxo)dicopper complex generated during the oxygenation of the Cu(I) starting material (performed with an excess of O_2) and the need for forceful purging of solutions of $Me_2L^{iPr,SX}CuO_2$ to induce bis(μ-oxo)dicopper complex formation suggests that there is an O_2 binding equilibrium characterized by very slow dissociation of O_2 (k_{off}) at −80 °C and a relatively large equilibrium constant (K_{eq}). This conclusion is supported by the magnitude of the computed free energy of oxygenation (−15.0 kcal/mol) for $Me_2L^{iPr,SMe}Cu$. According to this model, rapid purging is required so that the dissociated O_2 is removed from solution faster than it can be trapped by the generated Cu(I) species to reform $Me_2L^{iPr,SX}CuO_2$. Once the O_2 is removed, the Cu(I) species reacts irreversibly with the remaining $Me_2L^{iPr,SX}CuO_2$ to yield the bis(μ-oxo)dicopper intermediate. It is also possible that the vigorous bubbling slightly warms the solution, allowing for faster dissociation (k_{off}) and/or reaction to form the bis(μ-oxo)dicopper product.

In contrast, formation of a bis(μ-oxo)dicopper complex is not observed under any conditions for the systems ligated by $(R_2L^{iPr2})^-$.[19] Multiple possible effects of the thioether substituent

(48) Reliable computation of the energy difference between structures with bis(μ-oxo)dicopper(III) and (μ-η^2:η^2-peroxo)dicopper(II) cores has proven to be a difficult task. B3LYP and CASPT2 calculations have given conflicting results for the relative energies in model systems with three ammonia ligands per copper center.[48a] Delicate treatment of nondynamic electron correlation in the two isomers has been shown to be critical.[48a] Multireference configuration interaction (MRCI) methods have proved reliable, but are applicable only to the very smallest of models.[48b] A thorough comparison of the bis(μ-oxo) versus peroxo energy difference predicted by numerous hybrid and pure density functionals as compared to MRCI, completely renormalized coupled-cluster (CR−CC), and experimental results demonstrated that pure density functionals (and in particular BLYP) were considerably more accurate than their hybrid counterparts.[48c] This is largely due to nondynamic correlation making a larger contribution to the energy of the bis(μ-oxo)dicopper(III) core than to the (μ-η^2:η^2-peroxo)dicopper(II) core.[48a] Hybrid functionals, to the extent that they contain exact exchange, suppress the nondynamic correlation nonspecifically incorporated through the exchange functional, which detrimentally raises the relative energy of the bis(μ-oxo) form. Consequently, we applied the pure functional BLYP to the $[(Me_2L^{H,SMe}Cu)_2(\mu\text{-}O)_2]$ and $[(Me_2L^{H,SMe}Cu)_2(\mu\text{-}\eta^2\text{:}\eta^2\text{-}O_2)]$ structures here. If B3LYP is utilized instead, E_{solv} is computed to be 3.5 kcal/mol higher for the bis(μ-oxo) than the peroxo isomer, an error versus BLYP of 12.8 kcal/mol. This is consistent with the predictions from refs 48b and c that 5−7 kcal/mol of error should be expected per 10% Hartree−Fock (HF) exchange present in the hybrid functional (B3LYP contains 20% HF exchange). (a) Flock, M.; Pierloot, K. *J. Phys. Chem. A* **1999**, *103*, 95. (b) Rode, M. F.; Werner, H.-J. *Theor. Chem. Acc.* **2005**, *114*, 309. (c) Cramer, C. J.; Wloch, M.; Piecuch, P.; Puzzarini, C.; Gagliardi, L. *J. Phys. Chem. A* **2006**, *110*, 1991.

(49) Cramer, C. J.; Smith, B. A.; Tolman, W. B. *J. Am. Chem. Soc.* **1996**, *118*, 11283.

(50) ΔS for the dimerization reaction is estimated as follows. The assumption is first made that ΔS_{rot} and ΔS_{vib} are equal for the oxygenation and dimerization reactions. The translational entropy for dioxygen, $Me_2L^{iPr,SMe}Cu$, $Me_2L^{iPr,SMe}CuO_2$, and $[(Me_2L^{iPr,SMe}Cu)_2(\mu\text{-}O)_2]$ can be computed from statistical mechanics, leading to $\Delta S_{trans} = -36.1$ eu for the oxygenation reaction and $\Delta S_{trans} = -41.6$ eu for the dimerization reaction. The total ΔS for the oxygenation reaction (computed on the basis of vibrational frequency calculations for all species in this reaction) is −34.6 eu. The total ΔS for the dimerization reaction is then estimated to be −34.6 eu + $\Delta\Delta S_{trans} = -40$ eu.

in $(Me_2L^{iPr,SX})^-$ may be envisioned to underly these key differences in Cu/O_2 chemistry. By coordinating to the Cu(I) complex (a possibility supported by NMR, X-ray crystallographic, and DFT results, see above), the thioether may inhibit O_2 binding (decrease k_{on}), faciliate O_2 dissociation (increase k_{off}), or both. Any of these effects would result in a smaller K_{eq} as compared to the system supported by $(R_2L^{iPr2})^-$, for which O_2 binding is effectively irreversible at −80 °C. The reduced steric demand of the thioether arm in $(Me_2L^{iPr,SX})^-$ relative to the isopropyl substituent it replaces in $(R_2L^{iPr2})^-$ is also probably important, for such a reduction in size is necessary to access the rather compact bis(μ-oxo)dicopper core. Indeed, it is known that Cu(I) complexes of β-diketiminates that are less sterically hindered than $(R_2L^{iPr2})^-$ fail to yield observable 1:1 Cu/O_2 adducts and instead form bis(μ-oxo)dicopper species upon low-temperature oxygenation.[22] It is thus unusual to be able to observe both the 1:1 Cu/O_2 adduct and the bis(μ-oxo)dicopper complex as stable intermediates with a single supporting ligand system, further attesting to the novel properties of $(Me_2L^{iPr,SX})^-$.

(b) Reaction with PPh_3. The addition of 1 equiv of PPh_3 to a solution of $Me_2L^{iPr,SX}CuO_2$ that had been deoxygenated (by slow argon purge, to avoid bis(μ-oxo)dicopper complex formation) resulted in the gradual decay of the spectral features associated with the 1:1 Cu/O_2 adduct, with an approximate time to completion of 45 min for X = Me and 150 min for X = Ph as judged by UV−vis spectroscopy (THF, −80 °C, 0.5 mM). Characterization by ^1H and ^{31}P NMR spectroscopy of the products resulting from warming of the reaction solutions to room temperature indicated the formation of $Me_2L^{iPr,SX}Cu(PPh_3)$ (Scheme 1). Support for this assignment was obtained by comparison of the data to that acquired for an independently synthesized sample of $Me_2L^{iPr,SMe}Cu(PPh_3)$, which was structurally defined by X-ray crystallography (see above, Figure 4b). In the case of X = Me, the ^{31}P NMR data also showed a small amount of $OPPh_3$ (∼14% by integration), but no oxidized phosphine was observed in the case of X = Ph.

The finding that PPh_3 displaces O_2 from $Me_2L^{iPr,SX}CuO_2$ to yield a Cu(I) phosphine adduct parallels the results of the analogous reaction with $Me_2L^{iPr2}CuO_2$ (**2a**, R = Me), although the rates are significantly different.[36] At −80 °C, the parent complex $Me_2L^{iPr2}CuO_2$ is unreactive with PPh_3, and only yields the phosphine adduct upon warming, whereas conversion of the thioether-substituted system occurs at −80 °C. An associative mechanism was determined previously on the basis of kinetic data for the reaction of $Me_2L^{iPr2}CuO_2$ with the less hindered reagent $PMePh_2$.[36] Such an associative pathway may underly the faster rate of the reaction of PPh_3 with the thioether-substituted system, which is less sterically encumbered. Alternatively, thioether-induced pre-equilibrium loss of O_2 from $Me_2L^{iPr,SX}CuO_2$ (as proposed to occur upon argon purging, as described above) could provide $Me_2L^{iPr,SX}Cu$, which would then be trapped by PPh_3. The difference in rate between the ligands (X = Me > X = Ph) reflects their steric profiles, which would be expected to be manifested similarly in the associative and pre-equilibrium dissociative paths. Distinguishing between these possibilities will require extensive kinetic studies that have yet to be performed.

Conclusion

In summary, we have prepared two new ligands comprised of bidentate β-diketiminates with thioether substituents designed to model the N_2S(thioether) ligand set of the postulated catalytic "Cu_M" site of DβM and PHM. Copper(I) and (II) complexes of these ligands have been prepared and characterized. Intramolecular thioether coordination occurs in the monomeric Cu(II) compounds. In the case of one Cu(I) complex, X-ray crystallography indicates that a multinuclear structure is adopted in the solid state wherein the thioether group of a ligand bound to one copper ion binds to an adjacent metal center. Variable-temperature ^1H NMR studies of the Cu(I) compounds indicate complex behavior in solution, which we attribute to equilibria among species of varying nuclearity. Theoretical calculations support the notion of thioether coordination in mononuclear Cu(I) species that may be present in solution. Low-temperature oxygenation of solutions of the Cu(I) complexes generates stable 1:1 Cu/O_2 adducts, which on the basis of UV−vis and resonance Raman spectroscopic data and DFT calculations adopt side-on "η^2" structures with negligible Cu−thioether bonding and significant peroxo−Cu(III) character similar to previously reported analogues (**2a** and **2b**)[19] that lack the thioether group. In contrast to **2a** and **2b**, however, purging the solutions of the thioether-containing adducts with argon results in conversion to bis(μ-oxo)dicopper(III) species, identified as such by spectroscopy and theory. Loss of O_2 from the 1:1 Cu/O_2 adduct followed by rapid trapping of the product Cu(I) complex by remaining adduct rationalizes the formation of the bis(μ-oxo)-dicopper(III) complex. Thus, while the structure of the 1:1 Cu/O_2 adduct is not perturbed by the thioether substituent, the equilibrium constant for O_2 binding is decreased and bis(μ-oxo) complex formation is enabled when the thioether group is present.

The results reported herein provide precedence for a similar influence of the methionine ligand on the kinetics and/or thermodynamics of O_2 binding to the Cu_M site in DβM and PHM. Thus, the synthetic modeling work supports the notion[11,12] that the methionine ligand may disfavor O_2 binding, perhaps to prevent leakage of oxidizing equivalents and/or to control the timing of electron-transfer events. Recent theoretical calculations suggest that the methionine may also induce other effects, including preferential stabilization of an end-on geometry for a Cu/O_2 adduct in which the dioxygen moiety is less reduced than in the well-characterized synthetic side-on systems.[14] Testing of these notions through experiment remains an important goal for future research.

Experimental Section

General Considerations. All reagents were obtained from commercial sources and used without further purification, unless otherwise stated. The solvents THF, toluene, pentane, and Et_2O were dried over Na/benzophenone and distilled under nitrogen or passed through solvent purification columns (Glass Contour, Laguna, CA). All metal complexes were prepared and stored in a Vacuum Atmospheres inert atmosphere glovebox under a dry nitrogen atmosphere or were manipulated using standard inert atmosphere vacuum and Schlenk techniques. The copper reagents $(Me_3SiCH_2Cu)_4$[32] and $CuCl_2 \cdot 0.8THF$[51] were prepared according to literature procedures. 6-*i*Pr-2-Methylthiomethylaniline[25,26,52] and 2-(2,6-diisopropylphenylimido)-2-pentene-4-one[27] were prepared according to literature procedures. Labeled dioxygen was purchased from Cambridge Isotopes, Inc. or Icon Isotopes, Inc.

(51) So, J.-H.; Boudjouk, P. *Inorg. Chem.* **1990**, *29*, 1592.
(52) Note that this reaction is performed at −80 °C, not at 80 °C as stated in ref 25.

Physical Methods. NMR spectra were recorded on either Varian VI-300 or VXR-300 spectrometers. Chemical shifts (δ) for ^{1}H and ^{13}C NMR spectra are reported versus tetramethylsilane and were referenced to residual protium in the deuterated solvent. ^{31}P NMR spectra are referenced externally to 85% H_3PO_4. UV−vis spectra were recorded on an HP8453 (190−1100 nm) diode array spectrophotometer. Low-temperature spectra were acquired through the use of a Unisoko low-temperature UV−vis cell holder. When necessary, UV−vis spectra were corrected for drifting baselines due to minimal frosting of the UV cells caused by the low-temperature device. This was achieved by subtracting the average of a region with no absorbance (i.e., baseline, typically 950−1000 nm) from the entire spectrum. X-band EPR spectra were recorded on a Bruker E-500 spectrometer, with an Oxford Instruments EPR-10 liquid helium cryostat (4−20 K, 9.61 GHz). Quantitation of EPR signal intensity was accomplished by comparing the double integration of the derivative spectrum to that of H(Me_2L^{iPr2})CuCl[28] in 1:1 toluene/CH_2Cl_2. Resonance Raman spectra were collected on an Acton AM-506 spectrometer using a Princeton Instruments liquid N_2 cooled (LN1100-PB) CCD detector and ST-1385 controller interfaced with Winspec software. A Spectra-Physics BeamLok 2060-KR-V Krypton ion laser was used to excite at 406.7 or 457.9 nm. The spectra were obtained at −196 °C using a backscattering geometry; samples were frozen in a copper cup attached to a liquid nitrogen cooled coldfinger. Raman shifts were either externally referenced to liquid indene or internally referenced to solvent. Baseline corrections (polynomial fits) were carried out using Grams/32 Spectral Notebase Version 4.04 (Galactic). Elemental analyses were performed by Atlantic Microlab, Inc.

6-Isopropyl-2-phenylthiomethylaniline. This compound was prepared in a manner analogous to published procedures for 6-isopropyl-2-methylthiomethylaniline and related anilines.[25,26] Under nitrogen, dry CH_2Cl_2 (125 mL) was cooled to −80 °C in a 250 mL two-neck flask. To this were added 2-isopropylaniline (12 mL, 0.083 mol) and thioanisole (11 mL, 0.094 mol) while maintaining a temperature of −80 °C. *N*-Chlorosuccinimide (12.67 g, 0.095 mol) was added in portions over 30 min. The mixture was stirred and warmed to room temperature to yield a dark orange solution. Triethylamine (14.5 mL, 0.10 mol) was added, which caused the solution to turn very dark purple, and the mixture was then refluxed for 1 day. The reaction mixture was then cooled to room temperature and extracted with 10% w/v NaOH (2 × 250 mL). The combined organic layers were dried over Na_2SO_4, filtered, and the solvent was removed under reduced pressure to yield a dark red oil, which was purified by silica gel column chromatography (90:10 hexanes/ethyl acetate). Yield = 6.12 g (29%). ^{1}H NMR (300 MHz, $CDCl_3$): δ 7.38−7.20 (m, 5H), 7.10 (dd, J = 1.5, 7.8 Hz, 1H), 6.91 (dd, J = 1.5, 7.5 Hz, 1H), 6.70 (t, J = 7.8 Hz, 1H), 4.14 (s, 2H), 4.11 (br. s, 2H), 2.94 (heptet, J = 6.9 Hz, 1H), 1.27 (d, J = 6.9 Hz, 6H). ^{13}C{^{1}H} NMR (75 MHz, $CDCl_3$): δ 142.5, 136.3, 133.3, 130.3, 129.1, 128.6, 126.7, 125.2, 120.8, 118.6, 37.5, 27.9, 22.6. Anal. Calcd for $C_{15}H_{17}NS$: C, 74.66; H, 7.44; N, 5.44. Found: C, 74.20; H, 7.49; N, 5.38.

$Me_2L^{iPr,SMe}$H. Under nitrogen in a 250 mL two-neck flask equipped with a Dean Stark apparatus, 2-(2,6-diisopropylphenylimido)-2-pentene-4-one (5.49 g, 0.021 mol) and 6-isopropyl-2-methylthiomethylaniline (4.37, 0.022 mol) were dissolved in dry toluene (150 mL). Methanesulfonic acid (1.4 mL, 0.022 mol) was added, and the reaction mixture was refluxed under nitrogen overnight. Approximately 100 mL of toluene was removed by distillation before the remainder of the solvent was removed under reduced pressure. Approximately 100 mL of CH_2Cl_2 and 100 mL of saturated Na_2CO_3 were added to the resulting brown oil and stirred for 5 min. The layers were separated, and the aqueous layer was washed with CH_2Cl_2 (3 × 50 mL). The organics were combined and washed with 100 mL of saturated NaCl solution, then dried over anhydrous Na_2SO_4 and filtered. The solvent was removed from the filtrate under reduced pressure to yield an orange oil. EtOH was added (10 mL) and then removed under reduced pressure to yield an orange solid, which was further recrystallized from 75 mL of boiling EtOH. The volume was reduced to approximately 25 mL, and the solution was cooled to room temperature before placing in a −25 °C freezer. The resulting off-white crystals were isolated via vacuum filtration, washed with a minimal amount of cold EtOH (−80 °C), and dried in vacuo (2.74 g, 30%). Note: Despite repeated attempts at recrystallization, the crystalline product is a mixture of the desired product, $Me_2L^{iPr,SMe}$H, and the byproducts, Me_2L^{iPr2}H and Me_2L^{SMe2}H. Performing the reaction under nitrogen, as described above, optimizes the yield of product relative to byproducts to an approximate ratio of 6:3:1 by NMR spectroscopy. ^{1}H NMR (300 MHz, C_6D_6): δ 12.41 (s, 1H), 7.23−7.02 (m, 6H), 4.90 (s, 1H), 3.68 (d, J = 13.2 Hz, 1H), 3.58 (d, J = 13.2 Hz, 1H), 3.42−3.18 (m, 3H), 1.80 (s, 3H), 1.75 (s, 3H), 1.62 (s, 3H), 1.21−1.10 (m, 18H) ppm. ^{13}C{^{1}H} NMR (75 MHz, C_6D_6): δ 164.2, 159.4, 144.5, 144.3, 141.6, 138.5, 130.4, 127.2, 126.3, 124.7, 124.0, 123.4, 123.3, 123.2, 93.8, 35.5, 28.5, 28.4, 28.0, 24.7, 24.4, 24.3, 23.4, 23.3, 23.1, 21.7, 20.6, 15.8 ppm. HRESIMS: calcd for $C_{28}H_{41}N_2S$ ([M + H]$^+$), 437.2985. Found: m/z = 437.2987.

$Me_2L^{iPr,SPh}$H. Under nitrogen, a 250 mL two-neck flask was equipped with a Dean Stark apparatus, and 2-(2,6-diisopropylphenylimido)-2-pentene-4-one (5.54 g, 0.021 mol) and 6-isopropyl-2-phenyllthiomethylaniline (5.45 g, 0.021 mol) were dissolved in dry toluene (150 mL). Methanesulfonic acid (1.4 mL, 0.022 mol) was added, and the reaction mixture was refluxed under nitrogen overnight. Approximately 100 mL of toluene was removed by distillation before the remainder of the solvent was removed under reduced pressure. Approximately 100 mL of CH_2Cl_2 and 100 mL of saturated Na_2CO_3 were added to the resulting brown oil and stirred for 5 min. The layers were separated, and the aqueous layer was washed with CH_2Cl_2 (2 × 50 mL). The organics were combined and washed with 100 mL of saturated NaCl solution, then dried over anhydrous $MgSO_4$ and filtered. The solvent was removed from the filtrate under reduced pressure to yield a brown solid. MeOH was added (20 mL), and the mixture was stirred vigorously to yield a tan precipitate, which was isolated via vacuum filtration. The solid was recrystallized from 100 mL of boiling EtOH, allowed to cool to room temperature, and then stored at −4 °C. The resulting crystals were isolated and washed with cold EtOH (−80 °C) (3.50 g, 33%). ^{1}H NMR (300 MHz, C_6D_6): δ 12.46 (s, 1H), 7.40−6.90 (m, 11H), 4.90 (s, 1H), 4.21 (d, J = 12.4 Hz, 1H), 4.11 (d, J = 12.4 Hz, 1H), 3.35−3.18 (m, 3H), 1.81 (s, 3H), 1.61 (s, 3H), 1.21−1.14 (m, 9H), 1.12 (d, J = 6.9 Hz, 6H), 1.06 (d, J = 6.9 Hz, 3H) ppm. ^{13}C{^{1}H} NMR (75 MHz, C_6D_6): δ 165.0, 158.9, 145.1, 144.7, 144.6, 143.2, 141.2, 137.9, 137.7, 129.9, 129.1, 128.9, 127.4, 126.5, 126.2, 125.1, 124.0, 123.4, 123.3, 93.9, 36.3, 28.5, 28.0, 24.7, 24.6, 24.3, 23.3, 23.2, 23.0, 21.9, 20.5 ppm. Anal. Calcd for $C_{33}H_{42}N_2S$: C, 79.47; H, 8.49; N, 5.62. Found: C, 79.31; H, 8.47; N, 5.59.

$Me_2L^{iPr,SMe}$Li. A 2.5 M solution of ^{n}BuLi in hexane (0.58 mL, 1.45 mmol) was added to a stirring solution of the ∼ 6:3:1 mixture of $Me_2L^{iPr,SMe}$H and the byproducts Me_2L^{iPr2}H and Me_2L^{SMe2}H (0.630 g of the mixture, which corresponds to ∼0.380 g, ∼0.87 mmol of $Me_2L^{iPr,SMe}$H) in 5 mL of pentane. The desired product precipitated out of solution as a white solid, and the reaction mixture was allowed to stir for 1 h. The solid was collected via vacuum filtration and washed with cold pentane (0.369 g, ∼96% based on $Me_2L^{iPr,SMe}$H). ^{1}H NMR (300 MHz, C_6D_6): δ 7.26−7.12 (m, 4H), 6.92 (t, 1H), 6.72, (dd, J = 7.5, 1.5 Hz, 1H), 4.92 (s, 1H), 3.50−3.39 (m, 4H), 2.91 (d, J = 12.3 Hz, 1H), 1.89 (s, 3H), 1.80 (s, 3H), 1.31−1.19 (m, 21H) ppm. ^{13}C-{^{1}H} NMR (75 MHz, C_6D_6): 183.0, 165.3, 161.8, 150.8, 149.5, 142.2, 141.5, 141.2, 129.2, 126.3, 124.1, 123.8, 122.1, 93.5, 37.8, 28.5, 28.3, 28.1, 25.1, 25.0, 24.9, 24.8, 24.1, 23.7, 23.3, 23.0, 14.5 ppm.

$Me_2L^{iPr,SMe}$Cu. A solution of $Me_2L^{iPr,SMe}$Li (249 mg, 0.56 mmol) in 4 mL of THF was added to a slurry of CuCl (56.0 mg, 0.57 mmol) in 4 mL of THF. The solution immediately became bright yellow and was stirred for 1 h. The solvent was removed under reduced pressure, and the residue was extracted with ∼15 mL of pentane. The extract was filtered through Celite, and the solvent was then removed under

reduced pressure. The resulting yellow residue was stirred in pentane for 5 min. A yellow precipitate formed, which was isolated via vacuum filtration, washed with 5 mL of cold (−20 °C) pentane, and dried in vacuo (214 mg, 76%). ^{1}H NMR (300 MHz, C_6D_6): δ 7.27−7.15 (m, 4H), 6.88 (t, J = 7.5 Hz, 1H), 6.77 (d, J = 7.5 Hz, 1H), 4.88 (s, 1H), 3.66 (heptet, J = 6.6 Hz, 1H), 3.51−3.43 (m, 2H), 3.34 (heptet, J = 6.6 Hz, 1H), 3.15 (d, J = 11.4 Hz, 1H), 1.89 (s, 3H), 1.77 (s, 3H), 1.40 (d, J = 6.6 Hz, 3H), 1.31−1.27 (m, 12H), 1.18 (s, 3H), 1.09 (d, J = 6.9 Hz, 3H) ppm. UV−vis (THF) [λ_{max}, nm (ϵ, M^{-1} cm^{-1})]: (27 °C) 253 (sh, 16 700), 280 (sh, 11 200), 382 (19 500); (−80 °C) 255 (sh, 16 700), 280 (sh, 13 600), 357 (18 200), 382 (16 400). HRESIMS: calcd for $C_{28}H_{40}N_2Scu$, 499.2203 ([M + H]$^+$). Found: m/z = 499.2230. Anal. Calcd for $C_{28}H_{39}N_2SCu$: C, 67.36; H, 7.87; N, 5.61. Found: C, 66.99; H, 7.95; N, 5.30

$Me_2L^{iPr,SPh}Cu$. A solution of $Me_2L^{iPr,SPh}H$ (0.175 g, 0.35 mmol) in 5 mL of THF was added to solid $(Me_3SiCH_2Cu)_4$ (53.4 mg, 0.088 mmol) in a foil-wrapped vial. (Note: $(Me_3SiCH_2Cu)_4$ is light-sensitive; thus care must be taken to exclude excessive light.) The reaction mixture was stirred for 4.5 h and then filtered through Celite. The yellow filtrate was placed in a −20 °C freezer to precipitate the product as an off-white solid. The precipitate was collected via vacuum filtration, washed with ∼2 mL of cold pentane, and dried in vacuo (0.129 g, 65%). ^{1}H NMR (300 MHz, C_6D_6): δ 7.20−7.11 (m, 4H), 6.86 (d, J = 7.2 Hz, 2H), 6.79−6.64 (m, 4H), 6.43 (d, J = 6.9 Hz, 1H), 4.94 (s, 1H), 3.73−3.46 (m, 4H), 3.38 (septet, J = 6.6 Hz, 1H), 1.93 (s, 3H), 1.79 (s, 3H), 1.31−1.26 (m, 15H), 1.17 (d, J = 6.6 Hz, 3H) ppm. UV−vis (THF) [λ_{max}, nm (ϵ, M^{-1} cm^{-1})]: (27 °C) 242 (sh, 22 000), 282 (sh, 10 800), 380 (19 200); (−80 °C) 255 (sh, 15 600), 275 (sh, 13 300), 360 (16 300), 382 (15 200). HRESIMS: calcd for $C_{33}H_{42}N_2Scu$, 561.2359 ([M + H]$^+$). Found: m/z = 561.2345. Anal. Calcd for $C_{33}H_{41}N_2SCu$: C, 70.61; H, 7.36; N, 4.99. Found: C, 69.63; H, 7.48; N, 4.76.

$Me_2L^{iPr,SMe}CuCl$. A solution of $Me_2L^{iPr,SMe}Li$ (169 mg, 0.38 mmol) in 2 mL of THF was added to a slurry of $CuCl_2$·0.8THF (78.4 mg, 0.38 mmol) in 1 mL of THF. The solution turned dark brown/purple immediately. The reaction mixture was stirred for 4 h, and then the solvent was removed under reduced pressure. The resulting residue was dissolved in ∼8 mL of toluene and filtered through Celite. The volume of the filtrate was reduced to approximately 4 mL under reduced pressure, and approximately 3 mL of pentane was added to the solution. The mixture was then placed in a −20 °C freezer for 5−6 days to produce dark purple/brown crystals (94.4 mg, ∼46%).[53] X-ray quality crystals were grown from a 2:1 toluene/pentane solution. Note: The isolated single crystals contain a mixture of the desired product, as well as a byproduct, with a chlorine in the central methine position of the ligand backbone. UV−vis (CH_2Cl_2) [λ_{max}, nm (ϵ, M^{-1} cm^{-1})]: 279 (9000), 329 (16 700), 450 (1600), 577 (760), 850 (580). HRESIMS: calcd for $C_{28}H_{40}N_2SclCu$, 534.1891 ([M + H]$^+$). Found: m/z = 534.1894. HREIMS: calcd for $C_{28}H_{38}N_2SCl_2Cu$, 567.1429 (M$^+$). Found: m/z = 567.1411.

$Me_2L^{iPr,SPh}CuCl$. A 2.5 M solution of ^{n}BuLi in hexanes (0.16 mL, 0.40 mmol) was added to $Me_2L^{iPr,SPh}H$ (208 mg, 0.42 mmol) in ∼10 mL of pentane. The solution was stirred for 1 h. The solvent was then removed under reduced pressure to leave an orange residue. The residue was dissolved in ∼4 mL of THF and added to a slurry of $CuCl_2$·0.8THF (76.7 mg, 0.40 mmol) and stirred for 5 h. The solution became deep purple. The solvent was removed under reduced pressure, and the resulting residue was dissolved in ∼4 mL of toluene. The solution was filtered through Celite, and ∼4 mL of pentane was added and the mixture placed in a −20 °C freezer for 5−6 days. The resulting X-ray quality crystals were isolated and washed with pentane (112 mg, ∼47%).[53] Note: The isolated single crystals contain a mixture of the desired product, as well as a byproduct with a chlorine in the central methine position of the ligand backbone. UV−vis (CH_2Cl_2) [λ_{max}, nm (ϵ, M^{-1} cm^{-1})]: 275 (9200), 340 (15 900), 487 (1800), 598 (670), 875 (500). HRESIMS: calcd for $C_{33}H_{41}N_2SclCu$, 595.1970 (M$^+$). Found: m/z = 595.1983. HREIMS: calcd for $C_{33}H_{40}N_2SCl_2Cu$, 629.1585 (M$^+$). Found: m/z = 629.1627.

$Me_2L^{iPr,SMe}Cu(PPh_3)$. A solution of PPh_3 (22.3 mg, 0.085 mmol) in 2 mL of THF was added to a bright yellow suspension of $Me_2L^{iPr,SMe}$-Cu (42.6 mg, 0.085 mmol) in 4 mL of THF. The solution immediately bleached and became cloudy. After being stirred for 1 h, the mixture became clear and pale yellow. The solvent was then removed under reduced pressure to yield a sticky pale yellow residue. Repeated cycles of dissolution in pentane (∼2 mL) and subsequent evaporation under reduced pressure eventually yielded an off-white solid (2−3 repetitions) (30.0 mg, 46%). X-ray quality crystals were obtained by slow evaporation of a concentrated Et_2O solution at −20 °C. ^{1}H NMR (C_6D_6, 300 MHz): δ 7.26−6.87 (m, 21H), 5.16 (s, 1H), 3.91 (d, J = 13.5 Hz, 1H), 3.70−3.47 (m, 3H), 3.18 (d, J = 13.5 Hz, 1H), 1.97 (s, 3H), 1.87 (s, 3H), 1.73 (s, 3H), 1.28−1.22 (m, 9H), 0.98 (d, J = 6.9 Hz, 3H), 0.89−0.84 (m, 6H). ppm. ^{31}P{^{1}H} NMR (C_6D_6, 121.5 MHz): δ 3.79 ppm. Anal. Calcd for $C_{46}H_{54}CuN_2SP$: C, 72.55; H, 7.15; N, 3.68. Found: C, 72.79; H, 7.07, N, 3.67.

X-ray Crystallography. General Procedure. A crystal of appropriate size was placed on the tip of a 0.1 mm diameter glass capillary and mounted on either a Siemens or a Bruker SMART Platfrom CCD diffractometer for data collection at 173(2) K. The data collection was carried out using Mo Kα radiation (graphite monochromator) with an appropriate frame time for the size and quality of the crystal. A randomly oriented region of reciprocal space was surveyed to the extent of one sphere and to a resolution of either 0.84 or 0.77 Å. At least three major sets of frames were collected with 0.30° steps in ω at different ϕ settings and a detector position of −28° in 2θ. The intensity data were corrected for absorption and decay (SADABS).[54] Integration of the actual data was performed using SAINT.[55] The structure was solved using Sir97[56] (unless otherwise stated) and refined using SHELXL-97 (Sheldrick, 1997).[57] A direct methods solution was calculated, which provided most non-hydrogen atoms from the E-map. The remaining non-hydrogen atoms were located using full-matrix least squares/difference Fourier cycles. All non-hydrogen atoms were refined with anisotropic displacement parameters, unless stated otherwise. All hydrogen atoms were placed in ideal positions and refined as riding atoms with relative isotropic displacement parameters, unless stated otherwise. Further crystal and collection details are provided in the Supporting Information (CIF).

$Me_2L^{iPr,SPh}H$. X-ray quality crystals were grown from a concentrated EtOH solution. The N−H hydrogen was found by the E-map and refined accordingly. All other hydrogen atoms were placed in ideal positions and refined as riding atoms. Electron density corresponding to partial occupancy of hydrogen was found at both ligand nitrogen atoms, N1 and N2, indicating the hydrogen atom could reside at either nitrogen. In addition, each hydrogen electron density is within hydrogen-bonding distance of the other nitrogen. The hydrogen was thus modeled as disordered over two positions, H1 and H2, and refined to occupancies of 30% and 60%, respectively. The final full matrix least squares refinement converged to R1 = 0.0561 and wR2 = 0.1289 (F^2, all data).

$[Me_2L^{iPr,SMe}Cu]_4$. X-ray quality crystals were obtained from vapor diffusion of diethyl ether into a THF solution at −20 °C. Data collection was carried out on a Bruker Kappa SMART 6000 system at 100(1) K. The data collection was carried out using 0.4860 Å radiation (double-diamond monochromator) with a frame time of 1 s and a detector distance of 5.0 cm.[58] A randomly oriented region of reciprocal space

(53) This yield assumes no chloride incorporation in the backbone, although it is indicated by X-ray crystallography.

(54) An empirical correction for absorption anisotropy. Blessing, R. *Acta Crystallogr.* **1995**, *A51*, 33.
(55) *SAINT V6.2*; Bruker Analytical X-ray Systems: Madison, WI, 2001.
(56) Altomare, A.; Burla, M. C.; Cascarano, G.; Giacovazzo, C.; Guagliardi, A.; Moliterni, G. G.; Polidori, G.; Spagna, R. *J. Appl. Crystallogr.* **1998**, *32*, 115.
(57) *SHELXTL V6.10*; Bruker Analytical X-ray Systems: Madison, WI, 2000.
(58) Data were collected at APS ChemMatCARS 15-ID-C.

was surveyed to the extent of 2.0 hemispheres and to a resolution of 0.84 Å. Two sets of frames were collected with 0.30° steps in ω and one complete rotation of ϕ. The structure was solved using Bruker SHELXTL.[57] The structure consists of a tetramer of copper complexes. Only one-half of the tetramer is unique, with the other half generated by symmetry through an inversion center. There is a large librational motion of the isopropyl group (C42, C43, C44) about the C37−C42 bond, which causes disorder of the isopropyl group. This disorder was modeled by splitting these atoms into two parts with fixed 50/50 occupancy. The final full matrix least squares refinement converged to R1 = 0.0483 and wR2 = 0.1190 (F^2, all data).

$Me_2L^{iPr,SMe}CuCl$. X-ray quality crystals were grown from a 2:1 toluene/pentane mixture at −20 °C. This structure displays a minor compositional disorder in which the atom attached to C3 is either a hydrogen, as expected, or a chlorine (90:10, H:Cl). There is no other disorder in the main molecule. A toluene solvent molecule is present in the crystal structure; however, it is highly disordered and attempts to model it were unsuccessful. Thus, it was removed using the program PLATON/SQUEEZE.[59] A void volume of 858.3 Å^3 (with 196 electrons) out of a unit cell volume of 3378.1 Å, 25.4%, was found. The final full matrix least squares refinement converged to R1 = 0.0566 and wR2 = 0.1334 (F^2, all data).

$Me_2L^{iPr,SPh}CuCl$. X-ray quality crystals were grown from a 1:1 toluene/pentane solution at −20 °C. This structure displays a compositional disorder in which the atom attached to C3 is either a hydrogen, as expected, or a chlorine (53:47, H:Cl). There is no other disorder in the main molecule. The toluene solvent molecule contains a few large thermal ellipsoids. FLAT and DELU restraints were applied to the toluene to improve the model. However, further attempts to model the disorder did not lead to any improvement. The final full matrix least squares refinement converged to R1 = 0.0472 and wR2 = 0.1424 (F^2, all data).

$Me_2L^{iPr,SMe}Cu(PPh_3)$. X-ray quality crystals were obtained from evaporation of a diethyl ether solution at −20 °C. The structure was solved using SHELXS-97[57] and refined using SHELXL-97 (Sheldrick, 1997).[57] The final full matrix least squares refinement converged to R1 = 0.0503 and wR2 = 0.1201 (F^2, all data)

UV−Visible Absorption Spectroscopy. Formation of $Me_2L^{iPr,SX}CuO_2$. In a typical experiment, a 0.2−0.4 mM solution of $Me_2L^{iPr,SX}Cu$ in THF, toluene, or CH_2Cl_2 was placed in a UV cell in an inert atmosphere glovebox. The cuvette was sealed and brought out of the glovebox and cooled to −80 °C. The solution was oxygenated via bubbling excess dry O_2 for approximately 10 min, although the reaction is complete almost immediately.

Formation of $[(Me_2L^{iPr,SX}Cu)_2(\mu\text{-}O)_2]$. The 1:1 adduct, $Me_2L^{iPr,SX}CuO_2$, was prepared as described above (0.2−0.4 mM). Argon was then vigorously bubbled through the solution at −80 °C to produce the brown species, $[(Me_2L^{iPr,SX}Cu)_2(\mu\text{-}O)_2]$.

Resonance Raman Spectroscopy. Samples were prepared via the same protocols as described above for the UV−visible absorption spectroscopy experiments, except the initial Cu(I) concentrations were ∼10 mM. Samples for $^{18}O_2$-labeled resonance Raman experiments were prepared via freezing a solution of $Me_2L^{iPr,SX}Cu$ in a 10-mL Schlenk flask, evacuating the headspace, and vacuum transferring approximately 10 mL of $^{18}O_2$ gas. The Schlenk flask was then warmed to −80 °C with vigorous stirring to produce the mononuclear adducts, $Me_2L^{iPr,SX}CuO_2$. The $^{18}O_2$-labeled bis(μ-oxo) species, $(Me_2L^{iPr,SX}Cu)_2(\mu\text{-}O)_2$, was prepared via bubbling argon vigorously through this solution.

Reactivity Studies of $Me_2L^{iPr,SX}CuO_2$ with PPh_3. A solution of $H(Me_2L^{iPr,SX})Cu$ (ca. 2.6 mL, 10 mM)) in THF was placed in a 10 mL Schlenk flask under anaerobic conditions, cooled to −80 °C, and oxygenated by bubbling dry O_2 to produce a dark green solution of $Me_2L^{iPr,SX}CuO_2$. The solutions were deoxygenated by bubbling dry argon through the solution for ∼10 min. One equivalent of PPh_3 (0.22 mL, 120 mM) dissolved in THF was introduced via syringe (0.22 mL), and the solutions were stirred for 80 min at −80 °C. The color faded to yellow (X = Me) or orange (X = Ph). Upon warming to room temperature, further bleaching to pale yellow was observed. The solvent was removed under reduced pressure, and the resulting residue was dissolved in anaerobic and dry C_6D_6. $^{31}P\{^1H\}$ NMR (C_6D_6, 121.5 MHz) X = Me: δ 3.83 ($Me_2L^{iPr,SMe}Cu(PPh_3)$, 86%), 25.48 ($OPPh_3$, 14%) ppm. X = Ph: δ 3.94 ppm ($Me_2L^{iPr,SPh}Cu(PPh_3)$).

Computational Methods. (A) Density Functional Calculations. Geometry optimizations were carried out with the Jaguar suite, version 5.0, of ab initio quantum chemistry programs.[60] Because it has been demonstrated to be successful in predicting ligand−Cu(I) and −Cu(II) bond dissociation energies,[61] density functional theory (DFT) with the B3LYP functional[46] was used for geometry optimizations. Calculations were carried out at the restricted (RDFT) and unrestricted (UDFT) levels for singlet and triplet cases, respectively, according to the prescription identified in previous studies of 1:1 adducts of Cu(I) and dioxygen.[14,19c,d,20b] The lacvp** effective core potential basis[62] was used for Cu, while the double-ζ plus polarization (DZP) 6-31G** basis set was used for all other atoms.

Vibrational frequencies were calculated analytically and served to verify the B3LYP/DZP optimized geometries as minima. The calculations also enabled the determination of free energies by allowing for zero-point, enthalpy, and entropy corrections to be made. To optimize comparison of computed ν(O−O) values with those determined experimentally,[20] structures were reoptimized with B3LYP using the polarized triple-ζ (TZP) 6-311G** basis set on all atoms, except for Cu, for which the lacv3p** basis set (a triple-ζ basis compatible with the effective core potential)[62] was used. Frequencies at this level were scaled by 0.97 prior to reporting.[63] All vibrational frequency calculations were performed with a truncated ligand system for the sake of computational tractability: the three isopropyl groups are replaced with hydrogen atoms, and the positions of these atoms are optimized while holding the remainder of the structure fixed.

Single-point solvation energies for the optimized geometries were calculated using the self-consistent reaction field method as implemented in the Poisson−Boltzmann solver in Jaguar.[64] The dielectric constant ϵ for THF, which is used as the solvent for the purpose of comparison to experimental data, was taken to be 7.43 at 25 °C and 12.27 at −80 °C.[65] Computed gas-phase free energies for all species were converted from the 1 atm to the 1 M standard state by addition of a factor of $-RT^*\ln(A)$, where R is the universal gas constant and A is the molar volume of an ideal gas at 1 atm and a given temperature T.[66] Molar equilibrium concentrations for reactants and products in complexation reactions were computed from equilibrium constants determined as $K_{eq} = \exp(-\Delta G/RT)$.

(B) Multireference Calculations. Accurately modeling the open-shell singlet character of 1:1 adducts of Cu(I) and dioxygen, in particular those with a significant degree of Cu(II)−superoxo character, necessitates the use of methods beyond DFT. Although closed-shell singlet and high-spin triplet Kohn−Sham wave functions can be expressed as single Slater determinants, such open-shell singlet states are not a priori

(59) Spek, A. L. *Acta Crystallogr.* **1990**, *A46*, C34. Spek, A. L. PLATON, A Multipurpose Crystallographic Tool, Utrecht University, Utrecht, The Netherlands, 2000.

(60) *Jaguar 5.0*; Schrodinger, LLC: Portland, OR, 2002.
(61) Ducere, J.-M.; Goursot, A.; Berthomieu, D. *J. Phys. Chem. A* **2005**, *109*, 400.
(62) (a) Hay, P. J.; Wadt, W. R. *J. Chem. Phys.* **1985**, *82*, 270. (b) Wadt, W. R.; Hay, P. J. *J. Chem. Phys.* **1985**, *82*, 284. (c) Hay, P. J.; Wadt, W. R. *J. Chem. Phys.* **1985**, *82*, 299.
(63) Bauschlicher, C. W.; Partridge, H. *J. Chem. Phys.* **1995**, *103*, 1788.
(64) (a) Marten, B.; Kim, K.; Cortis, C.; Friesner, R. A.; Murphy, R. B.; Ringnalda, M. N.; Sitkoff, D.; Honig, B. *J. Phys. Chem.* **1996**, *100*, 11775. (b) Tannor, D. J.; Marten, B.; Murphy, R.; Friesner, R. A.; Sitkoff, D.; Nicholls, A.; Ringnalda, M.; Goddard, W. A.; Honig, B. *J. Am. Chem. Soc.* **1994**, *116*, 11875.
(65) (a) Carvajal, C.; Tolle, K. J.; Smid, J.; Szwarc, M. *J. Am. Chem. Soc.* **1965**, *87*, 5548. (b) Metz, D. J.; Glines, A. *J. Phys. Chem.* **1967**, *71*, 1158.
(66) Cramer, C. J. *Essentials of Computational Chemistry. Theories and Models*; John Wiley & Sons, Ltd.: West Sussex, England, 2002.

representable within the framework of Kohn−Sham DFT because they formally can only be expressed by at least two determinants. The multideterminantal nature of the 1:1 singlet adducts can be accounted for using single-point multireference second-order perturbation theory (CASPT2) calculations.[67,68] These computations also yield accurate singlet−triplet energy differences. The complete active space (CAS) for the reference wave function contains 18 electrons and 12 orbitals comprised from the Cu valence electrons/orbitals and the O_2 σ_{2p}, σ_{2p}*, π_{2p}, and π_{2p}* electrons/orbitals. Removal of orbitals with occupation numbers greater than 1.999 led to a final (12,9) active space. All CAS and CASPT2 calculations were carried out with the MOLCAS program.[69] A triple-ζ quality 17-electron relativistic effective core potential basis set was used for Cu,[70] and a TZP atomic natural orbital basis was used for S, O, N, and H(−N).[71] To keep calculations tractable, carbon was treated with the 3-21G basis[72] and H(−C) with the STO-3G basis.[73] As an additional step to facilitate these intensive calculations, a simplified version of the ligand system was used in which the backbone methyl groups and 2,6-diisopropylphenyl flanking groups (but retaining the thioether ligation to Cu) were transmuted to H atoms. The positions of these capping hydrogen atoms were optimized at the B3LYP/DZP level prior to CASPT2 calculations. The difference Δ (eq 1) in the relative energies of the singlet and triplet states at the DFT and CASPT2 levels was calculated for these small models. Assuming the triplet state is well represented within the DFT single-determinantal formalism, the relative energy difference between the triplet at the two levels of theory is negligible. The quantity Δ then becomes equal to the relative energy difference of the singlet state at the DFT and CASPT2 levels. By adding Δ to the DFT energies computed for the singlet states with the full model, final electronic energies, which then include an accounting for the multideterminantal character of the biradical singlet state, are obtained for the optimized structures with the full $(Me_2L^{iPr,SMe})^-$ ligand. This procedure has been shown to yield reliable energies for 1:1 $Cu-O_2$ adducts supported by similar ligand systems.[19c,d]

$$\Delta = ({}^1\mathrm{A} - {}^3\mathrm{A})_{\mathrm{CASPT2}} - ({}^1\mathrm{A} - {}^3\mathrm{A})_{\mathrm{DFT}} = [({}^1\mathrm{A})_{\mathrm{CASPT2}} - ({}^1\mathrm{A})_{\mathrm{DFT}}] - [({}^3\mathrm{A})_{\mathrm{CASPT2}} - ({}^3\mathrm{A})_{\mathrm{DFT}}] \quad (1)$$

Acknowledgment. We thank the NIH (GM47365 to W.B.T. and a NRSA postdoctoral fellowship to B.F.G.), the NSF (CHE-0203346 to C.J.C.), and the University of Minnesota (Lando-NSF Research Education for Undergraduates grant to N.H., Louise T. Dosdall Fellowship to N.W.A.) for providing financial support for this research. The APS ChemMatCARS 15-ID-C is principally supported by the National Science Foundation/ Department of Energy under grant CHE-0087817, and by the Illinois board of higher education. The APS is supported by the U.S. Department of Energy, Basic Energy Sciences, under Contract No. W-31-109-Eng-38. Finally, we thank L. Que, Jr. and J. Lipscomb for access to resonance Raman and EPR spectroscopy facilities and A. M. Reynolds for assistance with initial resonance Raman data acquisition.

Supporting Information Available: Additional figures and results of the theoretical calculations and X-ray crystallographic data (CIF). This material is available free of charge via the Internet at http://pubs.acs.org.

JA057745V

(67) Andersson, K.; Malmqvist, P. A.; Roos, B. O. *J. Chem. Phys.* **1992**, *96*, 1218.
(68) The situation is not the same for 2:1 adducts of copper and dioxygen, that is, the bis(μ-oxo)dicopper(III) and (μ-η^2:η^2-peroxo)dicopper(II) complexes. For discussion of CASPT2 versus DFT methods in these systems, see ref 48.
(69) Karlstrom, G.; Lindh, R.; Malmqvist, P. A.; Roos, B. O.; Ryde, U.; Veryazov, V.; Widmark, P. O.; Cossi, M.; Schimmelpfennig, B.; Neogrady, P.; Seijo, L. *Comput. Mater. Sci.* **2003**, *28*, 222.
(70) Barandiaran, Z.; Seijo, L. *Can. J. Chem.* **1992**, *70*, 409.
(71) Pierloot, K.; Dumez, B.; Widmark, P. O.; Roos, B. O. *Theor. Chim. Acta* **1995**, *90*, 87.
(72) Binkley, J. S.; Pople, J. A.; Hehre, W. J. *J. Am. Chem. Soc.* **1980**, *102*, 939.
(73) Hehre, W. J.; Stewart, R. F.; Pople, J. A. *J. Chem. Phys.* **1969**, *51*, 2657.